Applications and Applied Mathematics: An International Journal (AAM)

Volume 17 | Issue 2 Article 11

12-2022

(R1522) Modelling the Influence of Desertic Aerosols on the Transmission Dynamics of Neisseria Meningitidis Serogroup A

Francis Signing
University of Dschang; Sorbonne University

Berge Tsanou
University of Dschang; Sorbonne University

Samuel Bowong
University of Douala; Sorbonne University, samuelbowong@yahoo.fr

Available at
http://pvamu.edu/aam
Appl. Appl. Math.
ISSN: 1932-9466

Applications and Applied Mathematics:
An International Journal
(AAM)

Vol. 17, Issue 2 (December 2022), pp. 472 – 507

Modeling the Influence of Desert Aerosols on the Transmission Dynamics of Neisseria Meningitidis Serogroup A

[1,3,c]Francis Signing, [1,3,b]Berge Tsanou, and [2,3,a,*]Samuel Bowong

[1]Department of Mathematics and Computer Science, University of Dschang
P.O. Box 67, Dschang, Cameroon

[2]Laboratory of Mathematics, Department of Mathematics and Computer Science
Faculty of Science, University of Douala, PO Box 24157, Douala, Cameroon

[3]IRD, Sorbonne University, UMMISCO, F-93143, Bondy, France
[a]sbowong@gmail.com; [b]bergetsanou@gmail.com; [c]francis.signing@yahoo.fr

[*]Corresponding Author

Received: August 27, 2021; Accepted: April 20, 2022

Abstract

This paper assesses the role of desert aerosols and vaccine on the transmission dynamics of Neisseria Meningitis serogroup A (*NmA*). It is biologically well-documented that the inhalation of aerosol dust and its presence in the nasal cavity weakens the nasopharyngeal mucosa by damaging the mucosal barrier and inhibiting the mucosal immune defenses of susceptible and vaccinated individuals. We address the latter by proposing and analyzing a mathematical model for the dynamics of *NmA* that specifically accounts for the fast progression of susceptible and vaccinated individuals to the invasive stage of the disease. We compute the basic reproduction number and use it to investigate the existence and stability of equilibria. In this regard, we prove that the model undergoes a backward bifurcation phenomenon. We highlight the detrimental impact of aerosol dust by showing that its inhalation augments the reproduction number and enhances the endemic level of *NmA*. We also highlight the favorable role of vaccine in eliminating the disease when it has a high level of efficacy and is used to protect a large proportion of the population. The theoretical results are supported and illustrated by numerical simulations.

Keywords: Meningitis A; Aerosols; Fast progression; Vaccination; Global stability; Equilibrium; Awareness; Bifurcation; Nonlinear systems; Control measure; Reproduction number

MSC 2010 No.: 34A34, 34D23, 34D40, 92D30

1. Introduction

Meningitis is an inflammation of the meninges caused by different agents, the most common of which are bacterial or viral organisms. Meningococcal meningitis is a bacterial form of meningitis caused by a commensal bacterium of the human nasopharynx called *Neisseria meningitidis* (*Nm*). It is transmitted by nasopharyngeal secretions from healthy carriers to persons at risk (Tzeng et al. (2000)). He is a major cause of morbidity and mortality worldwide, with meningococcus being one of the infection agents (Teyssou and Muros-Le Rouzic (2007); WHO (2013); WHO (2010); WHO (2010); WHO (2009)). Nowadays, 13 serogroups of meningococcus are known (A, B, C, D, 29E, H, I, K, L, W, X, Y and Z), among which six (A, B, C, W, X and Y) are responsible for cases of invasive meningococcal disease worldwide (Boisier et al. (2007); Broomeet et al. (1983); Decosas and Koama (2002); Stephens et al. (2007)). Most cases are found in the battle zone called "African meningitis belt" (i.e., region extended from Senegal to Ethiopia, approximately populated by 250 million people) and in Asia, where epidemics are mainly caused by the Neisseria meningitis serogroup A (*NmA*) pathogen agent (Greenwood (1999); Lapeyssonnie (1963); Leimkugel et al. (2009); Molesworth et al. (2002)). Serogroups B and C of Neisseria meningitis (*NmB* and *NmC*) are the most common cause of meningococcal disease in Europe, Americas, Australia and New Zealand. Most people recover from meningitis if the treatment is initiated very early after the infection. However, permanent disabilities such as brain damage, hearing loss, and learning disabilities can result from the infection.

According the World Health Organization (WHO), the "African meningitis belt" registered the largest epidemic ever recorded in Africa in the year 1996 with more than 20,000 deaths and an approximate annual incidence rate of 1000 per 100,000 individuals (WHO (2013); WHO (2010); Trotter and Greenwood (2007)). Around 30 000 cases are still reported each year from that area. It has been well documented that seasonality is a strong determinant of meningococcal meningitis epidemics in the African belt, since during wet seasons, the endemic level of the incidence is around 0-0.5 per 100,000 per week in most health districts and cases tend to occur more frequently in winter and spring (Greenwood (1999); Mueller and Gessner (2010)). For instance, at the beginning of the dry season, there is a gradual increase in the number of cases until the beginning of the rains, when the incidence suddenly bounces back to its endemic level (Greenwood (1999)). More importantly, the incidence during this period of hyper-endemicity is of the order of 10-100 times the endemic incidence (Mueller and Gessner (2010)). The main hypothesis is that the particular weather conditions of the dry season in the African meningitis belt (very low relative humidity and dry winds of Harmattan laden with desert dust) would have weaken the nasopharyngeal mucosa of a colonized individual and increases its the risk of invasion by meningococci (Moore (1992)). This particular relevant characteristic of the disease should be incorporated in the mathematical modeling of the transmission dynamics of *NmA* if one wishes the resulted model to gain some more realism and provide insights into the understanding of *NmA* dynamics. For more details about the role of seasonality and its implications into the intra-seasonal variability of meningitis infection, we refer the reader to the works (Agier et al. (2013); Martiny and Chiapello (2013); Sultan et al. (2005)), where it is specifically shown that during dry season, the aerosol dust is the main cause of invasive meningococcal meningitis epidemics.

Due to the complex dynamics of *NmA*, the influence of seasonality through the presence of desert aerosols (dust) on its evolution, should be addressed alongside with the consideration of factors such as the population susceptibility to virulent serotypes and the spatial distribution of vegetation type (Alonso et al. (2006); Harrison et al. (2009); Teyssou and Muros-Le Rouzic (2007); Wilder-Smith and Memish (2003)). In fact, infection by *NmA* involves a sequence of three phenomena: (i) The carriage/portage phase, during which *NmA* normally colonize the upper respiratory tract without causing invasive disease. Individuals at this stage are referred to as healthy carriers or simply carriers; Under some favorable conditions, this process can occasionally lead to the development of invasive disease (Agier et al. (2013); Sultan et al. (2005)). (ii) The bacteremia phase, during which *NmA* manage to cross the blood-brain barriers and nasopharyngeal epithelium to invade the meninges. (iii) The invasive/septicemic phase, during which *NmA* induce the inflammation of meninges and eventually causes sepsis. Let us recall that sepsis is a serious condition resulting from the presence of harmful microorganisms in the blood or other tissues and the body's response to their presence potentially leading to the malfunctioning of various organs, shock, and death.

Early treatment with a range of antibiotics including penicillin, ampicillin and ceftriaxone is the most important measure to save lives and reduce complications. Moreover, antibiotic chemoprophylaxis for close contacts, when given promptly, decreases the risk of transmission. Prevention of bacterial meningitis can be achieved through vaccination and/or preventing contact with infectious individuals. Besides, there are three serogroup specific vaccines that confer varying degrees of duration of protection (Segal and Pollard (2004)).

Mathematical modeling and numerical simulations help to understand the dynamics of infectious diseases (Thieme (2003); Anderson and May (1992); Capasso (1993); Hethcote (2000)). A good understanding of the dynamics of *NmA* can result from the mathematical modeling which takes into consideration all the above mentioned features of the disease. This will certainly lead to extremely complicated mathematical systems to analyze due to the inherent complexity of such a generic consideration. So far, many researchers have modeled Neisseria meningitidis with excellent and promising ways of understanding the disease dynamic (Agusto and Leite (2019); Bah et al. (2019); Bowong et al. (2016); Asamoah et al. (2018); Bani-Yaghoub (2012); Bingen (2001); Bou Karam et al. (2009); Bornaa et al. (2015); Blyuss (2016); Djatcha Yaleu et al. (2017); Martcheva and Crispino-O'Connell (2003); Irving et al. (2012); Coen et al. (2000); Tuckwel et al. (2003); Stollenwerk and Jansen (2003); Trotter et al. (2005)). These mathematical models are mostly in the form of ordinary differential equations, age-structured systems which explicitly include, vaccination, treatment, healthy carriers or optimal control theory.

In order to pave the way for developing new more realistic models, we are motivated by the works in (Agier et al. (2013); Bah et al. (2019); Martiny and Chiapello (2013); Sultan et al. (2005); Djatcha Yaleu et al. (2017); Agusto and Leite (2019)). We therefore clear the ground by building on the most recent models by (Agusto and Leite (2019); Djatcha Yaleu et al. (2017)) by focusing on the impacts of desert aerosols (dust) on the transmission dynamics of *NmA*. In fact, it is well documented by many biological works that the inhalation of desert aerosols may enhance meningococcal invasion by damaging the mucosal barrier directly (irritating the epithelial lining

of the upper respiratory track) of susceptible individuals, allowing bacteria penetration, or by inhibiting mucosal immune defenses (Teyssou and Muros-Le Rouzic (2007); Alonso et al. (2006); Harrison et al. (2009); Wilder-Smith and Memish (2003)). This biological fact cannot be neglected in the mathematical modeling of the dynamical transmission of *NmA* within a human population and is accounted for in this paper.

The aim of this work is to provide a detailed analysis of the role of desert aerosols and vaccination in the spreading and the severity of *NmA* within a human population. As mentioned earlier, we first extend the models proposed in (Agusto and Leite (2019); Djatcha Yaleu et al. (2017)) by taking into account the inhalation of fine desert aerosols in ambient environments by susceptible and vaccinated individuals. We emphasize that the incorporation of desert aerosols in our model, via the presence of irritating aerosol dust in the nasal cavity weakens the nasopharyngeal mucosa of susceptible and vaccinated individuals. To the best of authors knowledge, the first (and probably the only) work which accounted for the role of desert aerosols on the dynamics of *NmA* is by (Bah et al. (2019)). However, in their model formulation, the authors have neglected the inhalation of desert aerosols by susceptible and vaccinated individuals which fasten their progression to the invasive stage of the disease. Rather, they have assumed that aerosol dust is inhalated only by asymptomatic carriers and promotes their progression to the invasive stage of *NmA*. The novelty of our modeling setting is therefore the role aerosol dust plays as a catalyzer of infection by accounting for the fast progression from susceptible and vaccinated individuals to the invasive stage of disease. We provide an in-depth theoretical study of the model in terms of the basic mathematical properties, existence and stability (local and global) of equilibria, bifurcation analysis, using the basic reproduction number as threshold or bifurcation parameter. In addition, we assess (analytically and numerically) the role of desert aerosols and vaccine on the transmission of *NmA* and find that:
(i) the basic reproduction number in the presence of desert aerosols is great than the basic reproduction number in the absence of desert aerosols.
(ii) At the endemic level, the number of infected individuals obtained in the presence of desert aerosols is larger than the corresponding number of infected individuals in the absence of desert aerosols.
(iii) A large vaccination coverage, with a high level of efficacy and the avoidance of the inhalation of desert aerosols can contribute to the reduction of *NmA* cases.

The remaining part of the paper is organized as follows. We build the mathematical model in Section 2 and conduct its theoretical analysis in Section 3. In Section 4, we assess the impact (favorable, detrimental) of desert aerosols and vaccine on the transmission dynamics of *NmA*. Some numerical simulations are provided throughout the manuscript to illustrate most of the theoretical results. Section 5 concludes the paper.

2. Model Formulation

Herein, we proceed with the construction of a mathematical model for the transmission dynamics of *NmA* within a human population, where people's nasal cavity and immune defenses are weak-

ened by desert aerosols which can irritate their throats and facilitate the penetrate of the bacteria *NmA* into the blood or brain streams.

2.1. Modeling context

Our baseline model follows (Agusto and Leite (2019); Djatcha Yaleu et al. (2017)). In order to shorten the expositions, the interested reader is therefore referred to (Agusto and Leite (2019); Djatcha Yaleu et al. (2017)) for more details on the model construction and assumptions of the baseline model in the absence of desert aerosols. We have kept as much as possible the same notations in (Agusto and Leite (2019); Djatcha Yaleu et al. (2017)) so that the reader can easily see that our model extends the works presented in (Agusto and Leite (2019); Djatcha Yaleu et al. (2017)) by accounting for the impact of aerosols dust. In fact, it is well known that the inhalation of aerosol dust and its presence in the nasal cavity weakens the nasopharyngeal mucosa of a colonized individual and triggers the four transmission events highlighted in the introduction section (Cartwright (1995); De Longueville et al. (2014); Deghmane and Taha (2010); Leimkugel et al. (2007)). Moreover, and contrary to (Bah et al. (2019)) our model accounts for fast and slow progressions of susceptible, vaccinated unprotected to the invasive stage of *NmA*. For the sake of simplicity, the extension is made possible by the introduction of a new class, say A, for the concentration of aerosols in the environment from which the dust that irritates the nasal cavity of persons at risk will be recruited. Note that A is actually not an epidemiological class, rather, it is a reservoir of aerosol dust. Furthermore, the newly introduced parameters will be contextualized and given, where necessary, with appropriate explanations.

2.2. Model parameters / variables and derivation of model equations

As mentioned earlier, we denote by A the concentration of desert aerosols into the troposphere at time t and, by μ_a the elimination rate of desert aerosols in the atmosphere. Once released from the earth surface, the aerosol particles rise into the troposphere (the lowest layer of the earth's atmosphere) under the action of turbulent mixing and upward convection currents. They are then transported by the winds for a varying time according to their size and the atmospheric conditions. We suppose that the desert aerosols are produced at rate Q per unit of time. Since wind erosion is accelerated by drought and, precipitation halts the production of dust, we suppose that the emission of desert aerosols is bounded. For convenience, we assume that the emission of aerosols into the troposphere converges to Q_* (i.e. $\lim\limits_{t\longrightarrow+\infty} Q(t) = Q_*$). Thus, the evolution of the concentration of desert aerosols into the troposphere is described by the following differential equation:

$$\dot{A} = Q_* - \mu_a A. \tag{1}$$

The total human population $N(t)$ at time $(t \geq 0)$ is a sum of susceptible $S(t)$, vaccinated $V(t)$, infectious $I(t)$ and recovered $R(t)$ individuals such that

$$N(t) = S(t) + V(t) + C(t) + I(t) + R(t). \tag{2}$$

Individuals are recruited into the population in the susceptible class at constant rate Λ. The population of vaccinated individuals is increased by the vaccination of susceptible individuals at a constant rate θ. Since the vaccine does not confer full immunity to all vaccine recipients, vaccinated individuals lose their protection and return to the susceptible class S at constant rate ω. Most of the theory about disease evolution is based on the assumption that the host population is homogeneous. Individual hosts, however, may differ and constitute very different habitats. In particular, some habitats may provide more resources or are more vulnerable to bacteria exploitation (Gandon et al. (2003)). The use of models with imperfect vaccines can better describe this type of human heterogeneity. Another explanation for the use of imperfect vaccines is that, it takes some time for individuals to acquire immunity after vaccination and in the meantime, a vaccinated individual can catch the infection. The vaccination can reduce, but may not completely prevent from acquiring to infection. Of course, an alternative approach to address the latter feature can the incorporation of time delay in the model and end up with a system of delayed differential equations. To keep a system of ordinary differential equations, we consider rather, a factor ν as the infection rate of vaccinated individuals so that, when $\nu = 0$, the vaccine is 100% effective, and when $\nu = 1$, the vaccine has no effect at all. The value $1-\nu$ can be understood as the inefficiency rate of the vaccine.

The transmission of *NmA* occurs in four different ways: (i) after adequate contacts with susceptible and infectious individuals, (ii) after adequate contacts with susceptible individuals and carriers, (iii) after adequate contacts with vaccinated unprotected and infectious individuals, (iv) after adequate contacts with vaccinated unprotected and carriers.

It is assumed that, in the presence of aerosols, compartments S and V encompass also individuals who have inhaled aerosols and those who did not. We model the aerosol rate of irritation (of the throat and nose cavity) by

$$\lambda_a = \frac{\beta_a A}{A + H}, \tag{3}$$

where, β_a is the effective ingestion/inhalation rate of desert aerosols by susceptible and vaccinated individuals. Overall, λ_a can be seen as a booster of the contact rate due to the presence of aerosol dust.

Hence, on the one hand, susceptible and vaccinated unprotected individuals, who have not yet inhaled aerosol dust become carriers at rates λ_h and $(1 - \nu)\lambda_h$, respectively, λ_h being the force of infection in the absence of the influence of aerosols and is modeled by

$$\lambda_h = \frac{\beta_h(\varepsilon C + I)}{N}. \tag{4}$$

In (4), β_h is the effective contact rate for *NmA* transmission, and $\varepsilon \geq 1$ is the modification parameter accounting the fact that carriers (those in the C class) are more infectious than infectious (those in the I class), because they are unidentified since they do not display any symptom.

On the other hand, susceptible and vaccinated unprotected individuals who have inhaled desert aerosols become infectious at rates $\lambda_a\lambda_h$ and $(1 - \nu)\lambda_a\lambda_h$, respectively. In fact, it is reasonable to postulate that healthy and vaccinated unprotected individuals who have already inhaled the desert aerosol and come into contact with the infected/carriers rapidly progress to the invasive

stage of *NmA* and their infection forces are boosted by the factor λ_a. A proportion p of susceptible individuals who are newly infected is assumed to develop the symptoms of the infection, while the complementary part $(1-p)$ becomes carriers. Also, we suppose that a fraction q of vaccinated unprotected individuals who are newly infected becomes infectious and the remainder $(1-q)$ enters the class of carriers. It is natural to assume that $p \geq q$, because the vaccination reinforces/boosts the immune system of vaccinated ones and therefore reduces their chances to progress rapidly to the infectious (invasive) stage of the disease. Practically, the fast progression pathway of *NmA* is described here by the direct flows from the susceptible (S) and vaccinated (V) classes, to the invasive stage (I) class.

Following the same reasoning as above, the carrier population is increased by susceptible and vaccinated individuals who caught the infection at rates $((1-p)\lambda_a + 1)\,\lambda_h$ and $((1-q)\lambda_a + 1)\,(1-\nu)\lambda_h$, respectively. Carriers are diminished by natural death at rate μ, progress to the infectious stage of the infection (moving to the class I) at rate γ, and recover from the infection (moving to the recovered class R) at rate α. The population of infectious is replenished following the infection of susceptible and vaccinated individuals at rates $p\lambda_a\lambda_h$ and $q(1-\nu)\lambda_a\lambda_h$, respectively. It diminishes by recovery from the infection (moving to the recovered class R) at rate δ, reduces by natural death and *NmA* induced death at constant rates μ and d, respectively. The population of recovered individuals is increased by the recovery of carriers and infectious at rates α and δ, respectively. It reduces due to natural mortality at rate μ.

We emphasize however that there are many possibilities to model the force of infection λ_h and the dynamics of A. For simplicity, we have chosen the formulations in (3) and (4).

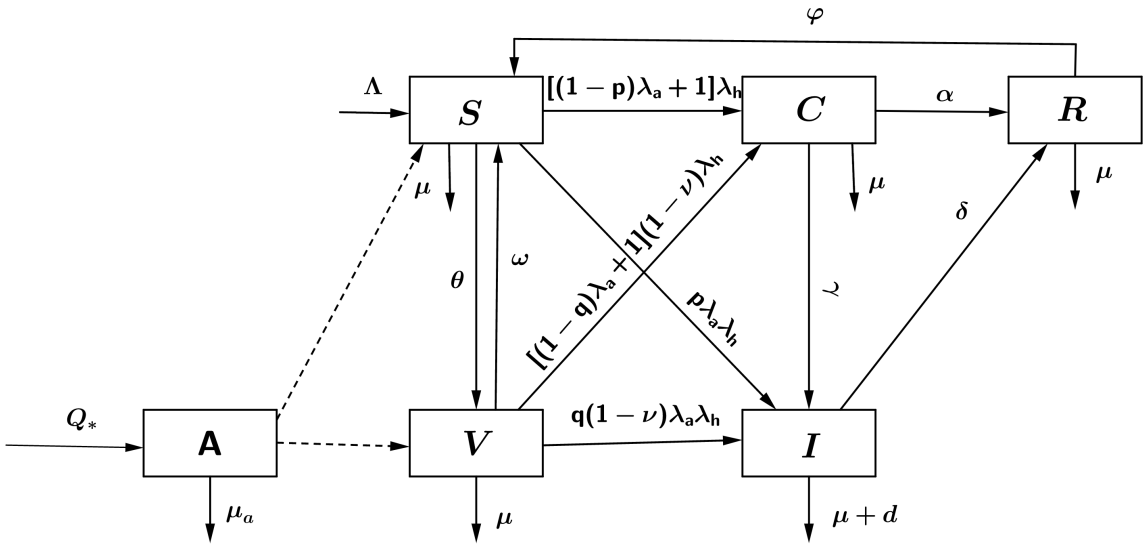

Figure 1. The schematic representation of the model (5). The dotted lines represent the dotted lines represent the ingestion of desert aerosols by susceptible and vaccinated individuals. The solid lines represent the transfers between and out the different compartments

Using the flowchart in Figure 1, we obtain the following deterministic system of nonlinear ordinary

differential equations:

$$\begin{cases} \dot{S} = \Lambda + \omega V - (\mu + \theta + (1+\lambda_a)\lambda_h)\, S + \varphi R, \\ \dot{V} = \theta S - (\omega + \mu + (1+\lambda_a)(1-\nu)\lambda_h)\, V, \\ \dot{C} = (((1-p)\lambda_a + 1)\, S + ((1-q)\lambda_a + 1)\,(1-\nu)V)\,\lambda_h - (\mu + \alpha + \gamma)\, C, \\ \dot{I} = (pS + q(1-\nu)V)\,\lambda_a\lambda_h + \gamma C - (\mu + d + \delta)I, \\ \dot{R} = \delta I + \alpha C - (\varphi + \mu)R, \\ \dot{A} = Q_* - \mu_a A. \end{cases} \tag{5}$$

Table 1 and Table 2 summarize the model variables and parameters values used for numerical simulations. For biological reasons, all the parameters are non-negative.

Table 1. Variables of system (5).

Symbol	Description	Unit	Symbol	Description	Unit
S	Susceptible individuals	indiv.	V	Vaccinated individuals	indiv.
C	Carriers	indiv.	I	Infectious	indiv.
R	Recovered individuals	indiv.	A	Concentration of aerosols	particle.m^{-3}

Table 2. Parameters values used for numerical simulations of system (5).

Symbol	Description	Unit	Estimate	Reference
Q_*	Emission rate of desert aerosols	particle.m^{-3}.day^{-1}	250	(Laurent et al. (2008))
Λ	Human recruitment rate	indiv. day^{-1}	3253607	(Agusto and Leite (2019))
θ	Vaccination coverage rate	day^{-1}	0.4868	(Agusto and Leite (2019))
μ	Natural mortality rate	day^{-1}	$1/56$	Assumed
δ	Recovery rate of infectious	day^{-1}	0.1128	(Agusto and Leite (2019))
d	*NmA* induced mortality rate	day^{-1}	0.63178	(Trotter et al. (2005))
β_h	*NmA* effective transmission rate	day^{-1}	Variable	Assumed
α	Rate of moving from carriers to recover	day^{-1}	0.1118	(Agusto and Leite (2019))
γ	Rate of moving from carriers to infected	day^{-1}	0.0438	(Agusto and Leite (2019))
μ_a	Desert aerosols depletion rate	particle.m^{-3}	0.2	(Bou Karam et al. (2009))
p	Fast progression proportion from S to I	dimensionless	0.45	Assumed
q	Fast progression proportion from V to I	dimensionless	0.25	Assumed
β_a	Inhalation rate of desert aerosols	dimensionless	Variable	Assumed
ν	Vaccine efficacy	dimensionless	0.85	(WHO (2009))
ε	Infectivity modification parameter	dimensionless	1.2	Assumed
H	Half saturation concentration of aerosols,	particle.m^{-3}	10^3	(Bou Karam et al. (2009))
ω	Waning rate of vaccine-induced immunity	day^{-1}	$0.7/365$	(CDC (2011); Hepkema et al. (2013))
φ	Waning rate of recovery-induced immunity	day^{-1}	0.63178	(Djatcha Yaleu et al. (2017))

From the last equation of system (5), one has that

$$\lim_{t \longrightarrow +\infty} A(t) = \frac{Q_*}{\mu_a} = A^0.$$

Thus, denoting $\lambda_a^0 = \beta_a A^0/(A^0 + H)$, the limiting system of (5) is given by

$$\begin{cases} \dot{S} = \Lambda + \omega V - (\mu + \theta + (1+\lambda_a^0)\lambda_h)\, S + \varphi R, \\ \dot{V} = \theta S - (\omega + \mu + (1+\lambda_a^0)(1-\nu)\lambda_h)\, V, \\ \dot{C} = (((1-p)\lambda_a^0 + 1)\, S + ((1-q)\lambda_a^0 + 1)\,(1-\nu)V)\,\lambda_h - (\mu + \alpha + \gamma)\, C, \\ \dot{I} = (pS + q(1-\nu)V)\,\lambda_a^0\lambda_h + \gamma C - (\mu + d + \delta)I, \\ \dot{R} = \delta I + \alpha C - (\varphi + \mu)R. \end{cases} \tag{6}$$

3. Analytical results

In this section, we proceed with the analytical results of system (6), by proving the global existence of a unique solution, studying the existence and asymptotic stability of equilibria and conducting a bifurcation analysis of the model.

3.1. Basic properties of the model

Herein, give the basic theoretical for results for system (6), which are essential for its well-posedness and shall be useful in the investigation of its long run dynamics.

Theorem 3.1.

System (6) is a dynamical system on the biologically feasible compact domain:

$$\Omega = \left\{ (S, V, I, C, R) \in \mathbb{R}^5_+, \quad N(t) \leq \frac{\Lambda}{\mu} \right\}. \tag{7}$$

Proof:

The proof is provided in two steps.

Step 1: We show that the solution variables $S(t), V(t),\ C(t),\ I(t)$ and $R(t)$ of system (6) at time $t > 0$, corresponding to non-negative initial conditions $S(0) > 0,\ V(0) \geq 0,\ C(0) \geq 0,\ I(0) \geq 0,$ $R(0) > 0$ are non-negative. To prove that, we define the quantity:

$$T = \sup \left\{ t > 0 / \forall z \in [0, t], S(z) > 0, \quad V(z) \geq 0, \quad I(z) \geq 0, \quad R(z) \geq 0 \right\}.$$

The existence of T follows by the continuity of the functions S, V, C, I, R, A and the standard Cauchy-Lipschitz theorem for ordinary differential equations. We must show that $T = +\infty$.

If $T = +\infty$ then, we are done.

Suppose by contradiction that, $T < +\infty$ (T finite). We are going to prove that $S(T) > 0, V(T) > 0, C(T) > 0, I(T) > 0$, and $R(T) > 0$. Without loss of generality we only show that $S(T) > 0$. In fact, from the first equation of system (6) one has

$$\dot{S}(t) + (\mu + \theta + (1 + \lambda_a)\lambda_h(t))\, S(t) - \Lambda = \omega V(t) + \varphi R(t). \tag{8}$$

By the definition of T above, we know that, for all $t \in [0, T]$, $\omega V(t) + \varphi R(t) \geq 0$. Thus,

$$\dot{S}(t) + (\mu + \theta + (1 + \lambda_a)\lambda_h(t))\, S(t) \geq \Lambda. \tag{9}$$

Denote the integrating factor of the right hand side of Equation (9) by

$$H_h(t) = \exp\left(\int_0^t (1 + \lambda_a)\lambda_h(s) ds + (\mu + \theta)t \right) > 0.$$

Then, from Equation (9), one has

$$\frac{d}{dt} \left[S(t) H_h(t) \right) \geq \Lambda H_h(t). \tag{10}$$

Integrating Equation (10) from 0 to T gives

$$\int_0^T \frac{d}{dt}\left[S(t)H_h(t)\right]dt = S(T)H_h(T) - S(0) \geq \Lambda \int_0^T H_h(t)dt.$$

Hence,

$$S(T) \geq \left[S(0) + \Lambda \int_0^T H_h(t)\right) \exp\left(-\int_0^T \lambda_h(s)ds - (\mu+\theta)T\right) > 0.$$

We have shown $S(t) > 0$ for all $t \in [0, T]$. Using the fact that $S(t) > 0$ for all $t \in [0, T]$, similar arguments can be used to prove that $V(t), C(t), I(t)$ and $R(t)$ are positive for all $t \in [0, T]$. We are going to prove that the later yields a contradiction. Consider the Cauchy problem of system (6) with the initial condition $S(T) > 0, V(T) > 0, C(T) > 0, I(T) > 0,\ R(T) > 0$. By classical the existence theorem for ordinary differential equations, there exists a solution v defined on an interval of the form $[T, T + \epsilon[,\ \epsilon > 0$. Therefore, the superposition of the latter and former solutions gives a solution of (6) which is defined and non-negative in an interval of the form $[T, T + \epsilon'[$, where $0 < \epsilon' < \epsilon$. This contradicts the fact that T is the supremum of the set $\left\{t > 0/\forall z \in [0, t], S(z) \geq 0,\ \ V(z) \geq 0,\ \ I(z) \geq 0,\ \ R(z) \geq 0\right\}$ is greater than T. Hence $T = +\infty$.

Step 2: The following boundedness property of $N(t)$

$$0 \leq N(0) \leq \frac{\Lambda}{\mu} \Longrightarrow 0 \leq N(t) \leq \frac{\Lambda}{\mu} \text{ for all } t \geq 0,$$

follows by summing up the equations of system (6) and applying Gronwall's inequality. Hence, the positive invariance of Ω.

The existence of the non-negative solution for all non-negative time t in *Step 1* and the positive invariance of Ω in *Step 2* achieve the proof of Theorem 3.1. ∎

The results of Theorem 3.1 ensures that system (6) is mathematically and epidemiologically well-posed, because every initial problem has a unique global solution and the state variables/population sizes are positive and can not grow exponentially.

In order to simplify some mathematical expressions, we adopt the following notations: $\Sigma = \beta_h/N$ and $\Sigma^0 = \beta_h/N^0$.

3.2. Global stability of the disease-free equilibrium

The disease-free equilibrium (DFE) for an epidemiological model is an equilibrium such that the disease is absent in the population. The DFE of system (6) is $E^0 = (S^0, V^0, C^0, I^0, R^0)$ with $C^0 = I^0 = 0$. It follows that $R^0 = 0$ and (S^0, V^0) is the solution of the following system:

$$\begin{cases} (\mu+\theta)S^0 - \omega V^0 = \Lambda, \\ \theta S^0 - (\mu+\omega)V^0 = 0. \end{cases} \tag{11}$$

Solving the above system of equations yields

$$S^0 = \frac{\Lambda(\mu+\omega)}{\mu(\omega+\mu+\theta)} \quad \text{and} \qquad V^0 = \frac{\Lambda\theta}{\mu(\omega+\mu+\theta)}. \tag{12}$$

Thus, the DFE of system (6) is

$$E^0 = \left(\frac{\Lambda(\mu+\omega)}{\mu(\omega+\mu+\theta)},\ \frac{\Lambda\theta}{\mu(\omega+\mu+\theta)},\ 0,\ 0,\ 0\right). \tag{13}$$

In order to study the local stability of the DFE E^0, we start by calculating the basic reproduction number $\mathcal{R}_0^{av}$. The basic reproduction number $\mathcal{R}_0^{av}$ is defined as the average number of secondary infections produced by one NmA-infected individual introduced into a susceptible population in the presence of desert aerosols.

For the calculation of $\mathcal{R}_0^{av}$, we apply the next generation method in (Diekmann et al. (1990); Diekmann et al. (2010); Van den Driessche and Watmough (2002)). Uninfected classes are those individuals who do not carry bacteria in their bodies (S, V), while infected classes are those individuals who carry bacteria in their bodies (C, I, R). The corresponding vector for the new infections $\mathcal{F}$, and the vector for the remaining transitions between compartments $\mathcal{V}$ for system (6) are given respectively by

$$\mathcal{F} = \begin{pmatrix} (((1-p)\lambda_a^0+1)\,S + ((1-q)\lambda_a^0+1)\,k_7V)\,\lambda_h \\ (pS+qk_7V)\,\lambda_a^0\lambda_h \\ 0 \end{pmatrix} \quad \text{and} \quad \mathcal{V} = \begin{pmatrix} D_1C \\ -\gamma C + D_2I \\ -\delta I - \alpha C + (\mu+\varphi)R \end{pmatrix},$$

where, $\lambda_a^0 = \beta_a A^0/(A^0+H)$ and $k_7 = 1-\nu$.

For the save of notation, we set once more:

$$D_3 = ((1-p)\lambda_a^0+1)\,S^0 + ((1-q)\lambda_a^0+1)\,(1-\nu)V^0, \quad N^0 = S^0+V^0 = \Lambda/\mu,$$
$$D_1 = \mu+\alpha+\gamma, \quad D_2 = \mu+d+\delta, \quad D_4 = (pS^0+q(1-\nu)V^0)\,\lambda_a^0.$$

The Jacobian matrices of $\mathcal{F}$ and $\mathcal{V}$ evaluated at the DFE E^0 are, respectively,

$$D\mathcal{F}(E^0) = \begin{pmatrix} \widetilde{F} & 0 \\ 0 & 0 \end{pmatrix} \quad \text{and} \qquad D\mathcal{V}(E^0) = \begin{pmatrix} \widetilde{V} & 0 \\ V_1 & V_2 \end{pmatrix},$$

where

$$\widetilde{F} = \begin{pmatrix} \varepsilon\Sigma^0 D_3 & \Sigma^0 D_3 \\ \varepsilon\Sigma^0 D_4 & \Sigma^0 D_4 \end{pmatrix} \quad \text{and} \qquad \widetilde{V} = \begin{pmatrix} D_1 & 0 \\ -\gamma & D_2 \end{pmatrix}.$$

Direct, but simple calculations yield

$$\widetilde{V}^{-1} = \begin{pmatrix} \dfrac{1}{D_1} & 0 \\ \dfrac{\gamma}{D_1D_2} & \dfrac{1}{D_2} \end{pmatrix} \quad \text{and} \quad \widetilde{F}\widetilde{V}^{-1} = \begin{pmatrix} \dfrac{\Sigma^0\,(\varepsilon D_2+\gamma)\,D_3}{D_1D_2} & \dfrac{\Sigma^0 D_3}{D_2} \\ \dfrac{\Sigma^0\,(\varepsilon D_2+\gamma)\,D_4}{D_1D_2} & \dfrac{\Sigma^0 D_4}{D_2} \end{pmatrix}.$$

By the definition in (Van den Driessche and Watmough (2002)), $F\widetilde{V}^{-1}$ is the next generation matrix. Observing that $\det\left(F\widetilde{V}^{-1}\right)=0$, we conclude that the basic reproduction number $\mathcal{R}_0^{av}$ of system (6), defined as the spectral radius of the next generation matrix is given by

$$\mathcal{R}_0^{av}=\frac{\Sigma^0\left(\left(\varepsilon D_2+\gamma\right)D_3+D_1D_4\right)}{D_1D_2}. \tag{14}$$

Now, we perform a sensitivity analysis to identify the most influential parameters on $\mathcal{R}_0^{av}$. The variation of $\mathcal{R}_0^{av}$ with respect a parameter ρ can be measured using the normalized sensitivity index $X_\rho^{\mathcal{R}_0^{av}}$, defined in (Bornaa et al. (2015); Kimaro et al. (2015)) by

$$X_\rho^{\mathcal{R}_0^{av}}=\frac{\partial\mathcal{R}_0^{av}}{\partial\rho}\times\frac{\rho}{\mathcal{R}_0^{av}}. \tag{15}$$

Since in this paper ρ and $\mathcal{R}_0^{av}$ are all positive, it follows that if $X_\rho^{\mathcal{R}_0^{av}}>0$, then $X_\rho^{\mathcal{R}_0^{av}}$ is an increasing function with respect to ρ, otherwise $X_\rho^{\mathcal{R}_0^{av}}$ is a decreasing function.

Using (15), the sensitivity indices of $\mathcal{R}_0^{av}$ are displayed in Table 3.

Table 3. Sensitivity indices for $\mathcal{R}_0^{av}$ when $\beta_h=0.3345$ and $\beta_a=0.573$.

Symbol	Sensitivity index	Symbol	Sensitivity index
Λ	0	θ	-0.2214521010
φ	0	μ	$+0.0906158663$
β_h	1	α	-0.4594162384
δ	-0.0155094364	d	-0.0868665933
γ	-0.3218591468	β_a	$+0.1946620003$
μ_a	-0.0865164445	ω	$+0.0144876492$
p	-0.0258843830	q	-0.0358195465
ν	-4.0899103920	ε	$+0.8938570195$
Q_*	$+0.0865164446$	H	-0.0865164446

The relevance of the basic reproduction number $\mathcal{R}_0^{av}$ relies on the following result.

Proposition 3.1.

The DFE point E^0 of system (6) is locally asymptotically stable in Ω if $\mathcal{R}_0^{av}<1$ and unstable if $\mathcal{R}_0^{av}>1$.

Proof:

The Jacobian matrix of system (6) evaluated at E^0 reads as

$$J\left(E^0\right)=\begin{pmatrix} -(\mu+\theta) & \omega & -\varepsilon\Sigma^0\left(1+\lambda_a^0\right)S^0 & -\Sigma^0\left(1+\lambda_a^0\right)S^0 & \varphi \\ \theta & -(\mu+\omega) & -\varepsilon k_7\left(1+\lambda_a^0\right)\Sigma^0V^0 & -k_7\left(1+\lambda_a^0\right)\Sigma^0V^0 & 0 \\ 0 & 0 & \varepsilon\Sigma^0D_3-D_1 & \Sigma^0D_3 & 0 \\ 0 & 0 & \varepsilon\Sigma^0D_4+\gamma & \Sigma^0D_4-D_2 & 0 \\ 0 & 0 & \alpha & \delta & -(\mu+\varphi) \end{pmatrix}. \quad (16)$$

The characteristic polynomial of $J\left(E^0\right)$ is

$$P(X)=-\left(X+\mu+\varphi\right)\left(X^2+\left(2\mu+\omega+\theta\right)X+\mu\left(\mu+\omega+\theta\right)\right)\left(X^2+TX+W\right),$$

where

$$T=\left(D_1+D_2\right)\left(1-\mathcal{R}_0^{av}\right)+\frac{\Sigma^0D_3\left(\varepsilon D_2+\gamma\right)}{D_1}+\frac{\Sigma^0\left(\gamma D_3+D_4D_1\right)}{D_2},\ W=D_2D_1\left(1-\mathcal{R}_0^{av}\right). \quad (17)$$

Classically, the local stability of E^0 depends on the signs of T and W. Thus, if $\mathcal{R}_0^{av}<1$, then $T,W>0$ and all the eigenvalues of $J\left(E^0\right)$ have negative real parts. Consequently, E^0 is locally asymptotically stable. If $\mathcal{R}_0^{av}>1$, then $W<0$ and there exists one positive eigenvalue of $J\left(E^0\right)$, implying that E^0 is unstable. This completes the proof. ■

For a better control of the disease, the global asymptotic stability (GAS) of the DFE E^0 is needed. Actually, enlarging the basin of attraction of E^0 to be the entire Ω is, for the model under consideration, a more challenging task and may require some additional thresholds besides $\mathcal{R}_0^{av}$ as shown in the following result.

Theorem 3.2.

Set $F_1=((1-p)\lambda_a^0+1)+((1-q)\lambda_a^0+1)(1-\nu)$ and $F_2=(p+q(1-\nu))\lambda_a^0$. Define

$$\xi_1=\frac{D_3\left(\varepsilon D_2+\gamma\right)+D_1D_4}{N^0\left(F_1\left(\varepsilon D_2+\gamma\right)+D_1F_2\right)}.$$

Then the DFE E^0 of system (6) is GAS if $\mathcal{R}_0^{av}\leq\xi_1<1$.

Proof:

We apply the method in Kamgang and Sallet (2008). In this regard, we write the system (6) in the following form:

$$\begin{cases}\dot{x}_1=A_1(x)(x_1-\overline{x}_0)+A_{12}(x)x_2,\\ \dot{x}_2=A_2(x)x_2,\end{cases} \quad (18)$$

where, $x=(x_1,x_2)^T$, $x_1=(S,V,R)^T$ represents the uninfected classes (the susceptible, vaccinated and recovered individuals), $x_2=(C,I)^T$ designates the infected classes (asymptomatic

carriers and infectious individuals), $\overline{x}_0 = (S^0, V^0, R^0)^T$,

$$A_1(x) = \begin{pmatrix} -(\theta+\mu) & \omega & \varphi \\ \theta & -(\omega+\mu) & 0 \\ 0 & 0 & -(\varphi+\mu) \end{pmatrix},\ A_{12}(x) = \begin{pmatrix} -\Sigma(1+\lambda_a^0)\varepsilon S & -\Sigma(1+\lambda_a^0)S \\ -\Sigma k_7(1+\lambda_a^0)\varepsilon V & -\Sigma k_7(1+\lambda_a^0)V \\ \alpha & \delta \end{pmatrix},$$

and

$$A_2(x) = \begin{pmatrix} \Sigma\varepsilon\left(k_5\lambda_a^0+1\right)S + \left(k_4\lambda_a^0+1\right)k_7V - D_1 & \Sigma\left(k_5\lambda_a^0+1\right)S + \left(k_4\lambda_a^0+1\right)k_7V \\ \Sigma\varepsilon\left(pS+qk_7V\right)\lambda_a^0 + \gamma & \Sigma\left(pS+qk_7V\right)\lambda_a^0 - D_2 \end{pmatrix},$$

with $k_4 = 1-q$ and $k_5 = 1-p$.

According to Kamgang and Sallet (2008), the DFE E^0 is globally asymptotically stable whenever the following five conditions are met:
H_1: The system (18) is defined on a positively invariant and dissipative subset Ω of $\mathbb{R}_+^{3+2}$.
H_2: The equilibrium point $\overline{x}_0$) for the sub-system $\dfrac{dx_1}{dt} = A_1(x_1,0)(x_1-\overline{x}_0)$, is globally asymptotically stable in the canonical projection of Ω in $\mathbb{R}_+^3$.
H_3: $A_2(x)$ is a Metzler (A Metzler matrix is a matrix with off-diagonal entries nonnegative (Smith and Waltman (1995))) and irreducible matrix for any given $x \in \Omega$.
H_4: There exists an upper-bound matrix $\overline{A}_2$ for the set $\Gamma = \{A_2(x), x \in \Omega\}$, with the property that either $\overline{A}_2 \notin \Gamma$ or if $\overline{A}_2 \in \Gamma$ (i.e., $\overline{A}_2 = \max_{\Omega}\Gamma$), then for any $\overline{x} \in \Omega$ such that $\overline{A}_2 = A_2(\overline{x})$, $\overline{x} \in \mathbb{R}_+^{n_1} \times \{0\}$ (i.e., the points where the maximum is realized are contained in the disease-free sub-manifold).
H_5: $\alpha(\overline{A}_2) \leq 0$, where $\alpha(\overline{A}_2)$ denotes the largest real part of the eigenvalues of $\overline{A}_2$.

We implement Theorem 4.3 in Kamgang and Sallet (2008) by showing that the requirements H_1 to H_5 are satisfied under the assumptions of Theorem 3.2.

The hypothesis H_1 follows readily from Theorem 3.1.

As for the hypothesis H_2, we rewrite the sub-system $\dot{x}_1 = A_1(x_1,0)(x_1-\overline{x}_0)$ as follows.

$$\begin{cases} \dot{S} = \Lambda + \omega V - (\theta+\mu)S + \varphi R, \\ \dot{V} = \theta S - (\omega+\mu)V, \\ \dot{R} = -(\varphi+\mu)R. \end{cases} \tag{19}$$

The hypothesis H_2 requires that the sub-system defined on $\Omega \bigcap \mathbb{R}_+^3$ be globally asymptotically stable in $\overline{x}_0$.

The system (19) can take the following compact form:

$$\dot{X}(t) = BX(t) + B_1, \tag{20}$$

where $X = (S, V, R)$,

$$B = \begin{pmatrix} -(\theta+\mu) & \omega & \varphi \\ \theta & -(\omega+\mu) & 0 \\ 0 & 0 & -(\varphi+\mu) \end{pmatrix} \quad \text{and} \quad B_1 = \begin{pmatrix} \Lambda \\ 0 \\ 0 \end{pmatrix}.$$

The three eigenvalues $-\mu, -(\mu+\varphi), -(\mu+\theta+\omega)$ of B are negative. Therefore, B is diagonalizable and there exists an invertible matrix P and a diagonal matrix D (whose diagonal entries are the eigenvalues of B) such that $D = P^{-1}BP$. Moreover, it is easy to prove that $X^* = -B^{-1}B_1 = (S^0, V^0, R^0)^T$ is the unique constant solution of Equation (20), and that classically, its general solution is given by

$$X(t) = X^* + Pe^{Dt}P^{-1}Y, \tag{21}$$

where, Y is a constant vector in $\mathbb{R}^3$ (depending on P and the initial conditions).

Since $\lim_{t\longrightarrow+\infty} e^{Dt} = 0$, we have $\lim_{t\longrightarrow+\infty} X(t) = X^* = (S^0, V^0, R^0)^T$. Thus, system (19) converges globally to $\overline{x}_0 = (S^0, V^0, R^0)^T$ and hypothesis H_2 is satisfied.

Observing that the two off-diagonal entries the matrix $A_2(x)$ are positive, irrespective of the values of its remaining entries, the associated directed graph of $A_2(x)$ is strongly connected. Thus, using Theorem 1.17 in Varga (1962), we conclude that $A_2(x)$ is an irreducible Metzler matrix. Hence, hypothesis H_3 is satisfied.

Now, we check the hypothesis H_4 by giving an upper bound of $A_2(x)$. First, note that for all $t \geq 0$, $S/N \leq 1$ and $V/N \leq 1$, so that an upper bound for $x \in \Omega$ is

$$\overline{A}_2 = \begin{pmatrix} \varepsilon\Sigma^0 N^0 F_1 - D_1 & \Sigma^0 N^0 F_1 \\ \varepsilon\Sigma^0 N^0 F_2 + \gamma & \Sigma^0 N^0 F_2 - D_2 \end{pmatrix},$$

where $F_1 = ((1-p)\lambda_a^0 + 1] + [(1-q)\lambda_a^0 + 1](1-\nu))$ and $F_2 = [p + q(1-\nu))\,\lambda_a^0$.

Note that $\overline{A}_2$ in not an element of Γ, so that hypothesis H_4 is satisfied.

Hypothesis H_5 requires that $\alpha(\overline{A}_2) \leq 0$ ($\overline{A}_2$ should be a stable Metzler matrix). Note that $\overline{A}_2$ is stable if and only if its determinant $\det(\overline{A}_2) \geq 0$ and its trace $\text{tr}(\overline{A}_2) \leq 0$. Thus, one has

$$-\Sigma^0 N^0 \left(F_1 \left(\varepsilon D_2 + \gamma\right) + D_1 F_2\right) + D_1 D_2 \geq 0 \quad \text{and} \quad \Sigma^0 N^0 \left(\varepsilon F_1 + F_2\right) - \left(D_1 + D_2\right) \leq 0.$$

Thus, $\overline{A}_2$ is stable if and only if

$$\frac{N^0 \left(F_1 \left(\varepsilon D_2 + \gamma\right) + D_1 F_2\right)}{D_3 \left(\varepsilon D_2 + \gamma\right) + D_1 D_4} \mathcal{R}_0^{av} \leq 1 \ \text{ and } \ \frac{N^0 \left(\varepsilon F_1 + F_2\right) D_1 D_2}{\left(D_1 + D_2\right)\left(D_3 \left(\varepsilon D_2 + \gamma\right) + D_1 D_4\right)} \mathcal{R}_0^{av} \leq 1. \tag{22}$$

We point out that the conditions in Equation (22) are equivalent to

$$\mathcal{R}_0^{av} \leq \xi_1 \qquad \text{and} \qquad \mathcal{R}_0^{av} \leq \xi_2, \tag{23}$$

where

$$\xi_1 = \frac{D_3 \left(\varepsilon D_2 + \gamma\right) + D_1 D_4}{N^0 \left(F_1 \left(\varepsilon D_2 + \gamma\right) + D_1 F_2\right)} \quad \text{and} \quad \xi_2 = \frac{\left(D_1 + D_2\right)\left(D_3 \left(\varepsilon D_2 + \gamma\right) + D_1 D_4\right)}{N^0 \left(\varepsilon F_1 + F_2\right) D_1 D_2}.$$

A simple calculation gives

$$\begin{aligned}\xi_1 - \xi_2 &= \frac{(D_3(\varepsilon D_2+\gamma)+D_1D_4)}{N^0}\left\{\frac{1}{(F_1(\varepsilon D_2+\gamma)+D_1F_2)} - \frac{D_1+D_2}{(\varepsilon F_1+F_2)D_1D_2}\right\}\\ &= -\frac{\left\{D_1(F_1\gamma+D_1F_2)+D_2F_1(\varepsilon D_2+\gamma)\right\}}{N^0(F_1(\varepsilon D_2+\gamma)+D_1F_2)(\varepsilon F_1+F_2)D_1D_2}.\end{aligned}$$

Since $\xi_1 - \xi_2 < 0$, then $\min\{\xi_1, \xi_2\} = \xi_1$. Thus $\overline{A}_2$ is a stable if

$$\xi_1 = \min\{\xi_1, \xi_2\} < 1. \tag{24}$$

Finally, since all the hypotheses $H_1 - H_5$ are satisfied, the application of Theorem 4.3 in Kamgang and Sallet (2008) implies that the DFE E^0 of system (6) is GAS in Ω if $\mathcal{R}_0^{av} \leq \xi_1 < 1$. This concludes the proof. ■

Figure 2 presents the phase portrait of system (6) when $\beta_h = 0.103345$ and $\beta_a = 0.11573$ (so that $\xi_1 = 0.1733875444$ and $\mathcal{R}_0 = 0.1284420311 < \xi_1 < 1$). It illustrates the global asymptotic stability of the DFE E^0. This means that meningitis disappears within the host population regardless of the initial condition of the system and the infection is controllable.

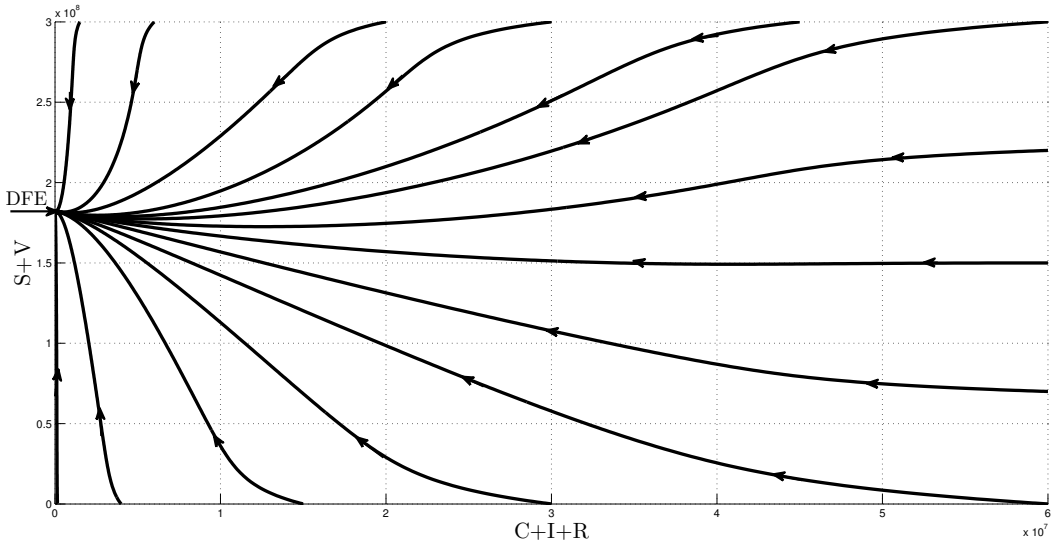

Figure 2. Global asymptotic stability of the DFE when $\mathcal{R}_0 \leq \xi_1 < 1$. Here, $\beta_h = 0.103345$ and $\beta_a = 0.11573$ (so that $\xi_1 = 0.1733875444$ and $\mathcal{R}_0 = 0.1284420311 < \xi_1 < 1$). All other parameter values are as in Table 2.

The result in Theorem 3.2 shows the (global) stability for the DFE only when $\mathcal{R}_0^{av} \leq \xi_1 < 1$. The existence of the additional threshold parameter ξ_1 for the global stability of DFE suggests the possibility that system (6) might exhibits a backward bifurcation. We shall address theoretically and numerically this phenomenon shortly.

3.3. Existence and stability of endemic equilibria

Herein, we investigate the existence and stability of endemic equilibrium points of system (6). An endemic equilibrium point of system (6), $E^{**} = (S^{**}, V^{**}, C^{**}, I^{**}, R^{**})$ is obtained by solving for positive solutions the following system:

$$\begin{cases} \Lambda + \omega V^{**} - (\theta + \mu + (1+\lambda_a^0)\lambda_h^{**})S^{**} + \varphi R^{**} = 0, \\ \theta S^{**} - (\omega + \mu + (1-\nu)(1+\lambda_a^0)\lambda_h^{**})\, V^{**} = 0, \\ (((1-p)\lambda_a^0 + 1)\, S^{**} + ((1-q)\lambda_a^0 + 1)\,(1-\nu)V^{**})\,\lambda_h^{**} - (\mu + \alpha + \gamma)\, C^{**} = 0, \\ (pS^{**} + q(1-\nu)V^{**})\,\lambda_a^0\lambda_h^{**} + \gamma C^{**} - (\mu + d + \delta)I^{**} = 0, \\ \delta I^{**} + \alpha C^{**} - (\varphi + \mu)R^{**} = 0, \end{cases} \tag{25}$$

where

$$\lambda_h^{**} = \frac{(\beta_h I^{**} + \varepsilon\beta_h C^{**})}{N^{**}},$$

is the force of infection evaluated at the endemic equilibrium point.

Straightforward but tedious computations give S^{**}, V^{**}, C^{**}, I^{**} and R^{**} in terms of λ_h^{**} as follows:

$$\begin{cases} C^{**} = \dfrac{e_{13}\,(\lambda_h^{**})^2 + e_{14}\lambda_h^{**}}{e_{10}\,(\lambda_h^{**})^2 + e_{11}\lambda_h^{**} + e_{12}},\ I^{**} = \dfrac{e_{15}\,(\lambda_h^{**})^2 + e_{16}\lambda_h^{**}}{e_{10}\,(\lambda_h^{**})^2 + e_{11}\lambda_h^{**} + e_{12}},\ R^{**} = \dfrac{\delta I^{**} + \alpha C^{**}}{\mu + \varphi}, \\ S^{**} = \dfrac{(\mu + \omega + (1+\lambda_a^0)(1-\nu)\lambda_h^{**})\,(\Lambda(\mu+\varphi) + \varphi\,(\delta I^{**} + \alpha C^{**}))}{(\mu+\varphi)\,\{(\mu + (1+\lambda_a^0)\lambda_h^{**})\,(\mu + \omega + (1+\lambda_a^0)k_7\lambda_h^{**}) + \theta\,[\mu + (1+\lambda_a^0)k_7\lambda_h^{**})\}}, \\ V^{**} = \dfrac{\theta\,(\Lambda(\mu+\varphi) + \varphi\,(\delta I^{**} + \alpha C^{**}))}{(\mu+\varphi)\,\{(\mu + (1+\lambda_a^0)\lambda_h^{**})\,(\mu + \omega + (1+\lambda_a^0)k_7\lambda_h^{**}) + \theta\,[\mu + (1+\lambda_a^0)k_7\lambda_h^{**})\}}, \end{cases} \tag{26}$$

where

$$\begin{aligned} e_{10} = {} & k_7\left(1+\lambda_a^0\right)\left\{\,\mu^3 + (\,\gamma + \alpha + d + \delta + \varphi)\,\mu^2 + [(d+\varphi+\delta)\,\gamma + \alpha\,d + \alpha\,\delta + d\varphi + \delta\,\varphi]\,\mu\right. \\ & + \gamma d\varphi + \lambda_a^0\big[\mu^3 + p\alpha\,\varphi\,d + \gamma d\varphi + [(d+\varphi+\delta)\,\gamma + \alpha\,d + \alpha\,\delta + d\varphi + p\alpha\,\varphi + k_5\delta\,\varphi]\,\mu \\ & \left. + (\,\gamma + \alpha + d + \delta + \varphi)\,\mu^2\big]\right\}, \end{aligned}$$

$$\begin{aligned} e_{11} = {} & \mu^4 + (\,\gamma + \omega + d + \delta + \varphi + \alpha)\,\mu^3 + \big[\,(d + \omega\ + \varphi + \delta)\,\gamma + \omega\,\delta + \delta\,\varphi + \omega\,\alpha + d\varphi + \omega\,\varphi \\ & + \omega\,d + \alpha\,d + \alpha\,\delta\big]\mu^2 + [(\omega\,\delta + \omega\,d + \omega\,\varphi + d\varphi)\,\gamma + \omega\,d\varphi + \omega\,\delta\,\varphi + \omega\,\alpha\,d + \omega\,\alpha\,\delta]\,\mu \\ & + \omega\ \gamma d\varphi + \big\{\mu^4 + (\,\gamma + \omega + d + \delta + \varphi + \alpha)\,\mu^3 + \big[\,(d + \omega\ + \varphi + \delta)\,\gamma + p\alpha\,\varphi + k_5\delta\,\varphi \\ & + \omega\,\varphi + \alpha\,d + \omega\,\delta + \omega\,d + \omega\,\alpha + d\varphi + \alpha\,\delta\big]\mu^2 + \big[\,(\omega\,\delta + \omega\,d + \omega\,\varphi + d\varphi)\,\gamma + \omega\,\alpha\,d \\ & + p\alpha\,\varphi\,d\ + k_5\delta\,\varphi\,\omega + p\omega\,\alpha\,\varphi + \omega\,\alpha\,\delta + \omega\,d\varphi\big]\mu + \omega\ \gamma d\varphi + p\omega\,\alpha\,\varphi\,d\big\}\lambda_a^0 + \big\{\mu^4 + (\,\gamma + \alpha \\ & + \delta\ + \varphi + d + \theta)\mu^3 + \big[\,(\varphi + d + \theta\ + \delta)\,\gamma + \alpha\,d + d\varphi + \theta\,\delta + \theta\,d + \theta\,\varphi + \alpha\,\varphi + \alpha\,\delta \\ & + \theta\,\alpha + \delta\,\varphi\big]\mu^2\ + \big[\theta\,d\varphi + \alpha\,\delta\,\varphi + \alpha\,d\varphi + \theta\,\alpha\,d + \theta\,\delta\,\varphi + \theta\,\alpha\,\delta + (d\varphi + \theta\,\varphi + \theta\,d + \delta\,\varphi \\ & + \theta\,\delta)\gamma\big]\mu + \theta\ \gamma d\varphi\ + \big[\mu^4 + \theta\ \gamma d\varphi + \theta\,q\alpha\,\varphi\,d + (\,\gamma + \alpha + \delta + \varphi + d + \theta)\,\mu^3 + \big[(\varphi + d \\ & + \theta\ + \delta)\gamma + \alpha\,d + d\varphi + \theta\,\delta + \theta\,d + \theta\,\varphi + \alpha\,\varphi + \alpha\,\delta + \theta\,\alpha + \delta\,\varphi\big]\mu^2 + \big((d\varphi + \theta\,\varphi + \theta\,d \\ & + \delta\,\varphi + \theta\,\delta)\gamma + \theta\,q\alpha\,\varphi + \alpha\,\delta\,\varphi + \alpha\,d\varphi + \theta\,d\varphi + \theta\,\delta\,\varphi(1-q) + \theta\,\alpha\,d + \theta\,\alpha\,\delta\big)\mu\big]\lambda_a^0\big\}k_7, \end{aligned}$$

$$
\begin{aligned}
e_{12} &= \mu\,(\mu+\varphi)(\,\mu+\omega+\theta)\,D_1\,D_2,\\
e_{13} &= \Lambda\,D_2(\,\mu+\varphi)(1+\lambda_a^0)\left((1-p)\,\lambda_a^0+1\right)(1-\nu),\\
e_{14} &= \Lambda(\,\mu+\varphi)D_2\left\{\theta\left((1-q)\,\lambda_a^0+1\right)(1-\nu)+\left((1-p)\,\lambda_a^0+1\right)(\,\mu+\omega)\right\},\\
e_{15} &= \Lambda(\,\mu+\varphi)(1-\nu)(1+\lambda_a^0)\left\{\left((1-p)\,\lambda_a^0+1\right)\,\gamma+p\,\lambda_a^0\,D_1\right\},\\
e_{16} &= \Lambda(\,\mu+\varphi)\Big\{\,\gamma\Big\{\left((1-p)\,\lambda_a^0+1\right)(\,\mu+\omega)+\theta\left((1-q)\,\lambda_a^0+1\right)(1-\nu)\Big\}\\
&\quad+(p(\,\mu+\omega)+q(1-\nu)\,\theta)\;\lambda_a^0 D_1\Big\}.
\end{aligned}
$$

Note that at the endemic equilibrium state E^{**}, one has

$$N^{**}=\frac{\Sigma^0 N^0\,(I^{**}+\varepsilon C^{**})}{\lambda_h^{**}}=\frac{\Lambda}{\mu}-\frac{dI^{**}}{\mu}. \tag{27}$$

Equation (27) reduces to

$$\left(\mu\Sigma^0 N^0+d\lambda_h^{**}\right)I^{**}+\mu\varepsilon\Sigma^0 N^0 C^{**}-\Lambda\lambda_h^{**}=0. \tag{28}$$

Now, after replacing in (28) I^{**} and C^{**} by their expressions given in Equation (26), one obtains the quadratic equation

$$e_{19}\,(\lambda_h^{**})^2+e_{20}\lambda_h^{**}+e_{21}=0, \tag{29}$$

where

$$
\begin{cases}
e_{19}=\mu\,\Lambda\;(1-\nu)\,(1+\lambda_a^0)\left\{\left[\,(\delta+\varphi+\gamma+d(1-p)+\alpha)\,\mu+p\alpha\,\varphi+\alpha\,\delta+(1-p)\,(\alpha\,d\right.\right.\\
\qquad\left.+d\varphi+\delta\,\varphi)+\mu^2+\gamma\;(\varphi+\delta)\,\right]\lambda_a^0+\mu^2+(d+\delta+\varphi+\alpha+\gamma)\,\mu+\gamma\,(\varphi+\delta)\\
\qquad\left.+d\varphi+\alpha\,d+\alpha\,\delta+\delta\,\varphi\right\},\\
e_{20}=-\mu\Sigma^0 N^0 e_{15}-de_{16}-\mu\varepsilon\Sigma^0 N^0 e_{13}+\Lambda e_{11},\\
e_{21}=\Lambda\mu(\mu+\varphi)D_1D_2(\mu+\omega+\theta)\,(1-\mathcal{R}_0^{av})\,.
\end{cases} \tag{30}
$$

The number of possible real solutions of Equation (29) is determined by the sign of the coefficients e_{19}, e_{20} and e_{21}. Thus, define $g(\lambda_h^{**})=e_{19}\,(\lambda_h^{**})^2+e_{20}\lambda_h^{**}+e_{21}$ and use Descartes' Rule of Signs to decide on the number of positive roots of g. That result is given in Table 4.

Table 4. The number of possible positive roots for Equation (28).

$\mathcal{R}_0^{av}$	Sign of e_{19}	Sign of e_{20}	Sign of e_{21}	Number of sign changes	Number of possible endemic equilibria
$\mathcal{R}_0^{av}>1$	+	-	-	1	1
	+	+	-		
$\mathcal{R}_0^{av}<1$	+	-	+	2	0 or 2
	+	+	+	0	0

The following result summarizes the existence of endemic equilibrium points of system (6).

Theorem 3.3.

The following statements hold:

(1) System (6) does not have an endemic equilibrium in either of the following three cases:

(i) $\mathcal{R}_0^{av} = 1$ and $e_{20} > 0$.
(ii) $\mathcal{R}_0^{av} < 1$, $e_{20}^2 - 4e_{19}e_{21} > 0$ and $e_{20} > 0$.
(iii) $\mathcal{R}_0^{av} < 1$ and $e_{20}^2 - 4e_{19}e_{21} < 0$.

(2) The meningitis model (6) has a unique endemic equilibrium in either of the following three cases:

(i) $\mathcal{R}_0^{av} > 1$, and Equation (26) has the unique solution:

$$\lambda_h^{**} = \frac{-e_{20} + \sqrt{(e_{20})^2 - 4e_{21}e_{19}}}{2e_{19}}. \tag{31}$$

(ii) $\mathcal{R}_0^{av} < 1$, $e_{20}^2 - 4e_{19}e_{21} = 0$ and $e_{20} < 0$, and the corresponding unique solution of Equation (26) is $\lambda_{h_0}^{**} = \dfrac{-e_{20}}{2e_{1i}}$.

(iii) $\mathcal{R}_0^{av} = 1$ and $e_{20} < 0$, Equation (26) has the unique solution given by $\lambda_{h_3}^{**} = \dfrac{-e_{20}}{e_{19}}$.

(3) System (6) has two endemic equilibria given by (26) if $\mathcal{R}_0^{av} < 1$, $e_{20}^2 - 4e_{19}e_{21} > 0$ and $e_{20} < 0$. The corresponding forces of infection which are two solutions of Equation (26) read:

$$\lambda_{h_1}^{**} = \frac{-e_{20} + \sqrt{(e_{20})^2 - 4e_{21}e_{19}}}{2e_{19}} \quad \text{and} \quad \lambda_{h_2}^{**} = \frac{-e_{20} - \sqrt{(e_{20})^2 - 4e_{21}e_{19}}}{2e_{19}}.$$

The combination of Theorem 3.2 and Theorem 3.3 indicates the possibility of forward and backward bifurcation phenomena (Dushoff et al. (1998); Carr (1981); Brauer (2004); Garba et al. (2008); Sharomi et al. (2007); Xu (2013); Xu and Liao (2014); Xu and Li (2015)). This is the phenomenon where the disease-free equilibrium co-exist with a stable endemic equilibrium when the associated reproduction number $\mathcal{R}_0^{av}$ is less than one. The local asymptotic stability of the unique endemic equilibrium $E^{**} = (S^{**}, V^{**}, C^{**}, I^{**}, R^{**})$ when $\mathcal{R}_0^{av} > 1$, the existence of a forward bifurcation around E^{**} at $\mathcal{R}_0^{av} = 1$, as well as the existence of backward bifurcation at $\mathcal{R}_0^{av} = 1$ suggested by Theorem 3.2 and Theorem 3.3 are confirmed by Theorem 3.4 below. Its proof which uses the Center Manifold Theory (Carr (1981); Castillo-Chavez and Song (2004)) is provided in Appendix A and is numerically illustrated in Figure 3.

Theorem 3.4.

Let $\mathcal{A}$ be the quantity given by Equation (45) in Appendix A. If $\mathcal{A} > 0$, then system (6) undergoes a backward bifurcation at $\mathcal{R}_0^{av} = 1$. If $\mathcal{A} < 0$, then system (6) exhibits a forward bifurcation at $\mathcal{R}_0^{av} = 1$. Moreover, the unique endemic equilibrium point E^{**} is LAS whenever $\mathcal{R}_0^{av} > 1$, but close to 1.

The results of Theorem 3.4 are similar to those in Agusto and Leite (2019), Djatcha Yaleu et al. (2017), and Bah et al. (2019). In such a scenario, the classical requirement of the basic reproduction number being less than the unity is only a necessary, but not a sufficient condition for the disease elimination.

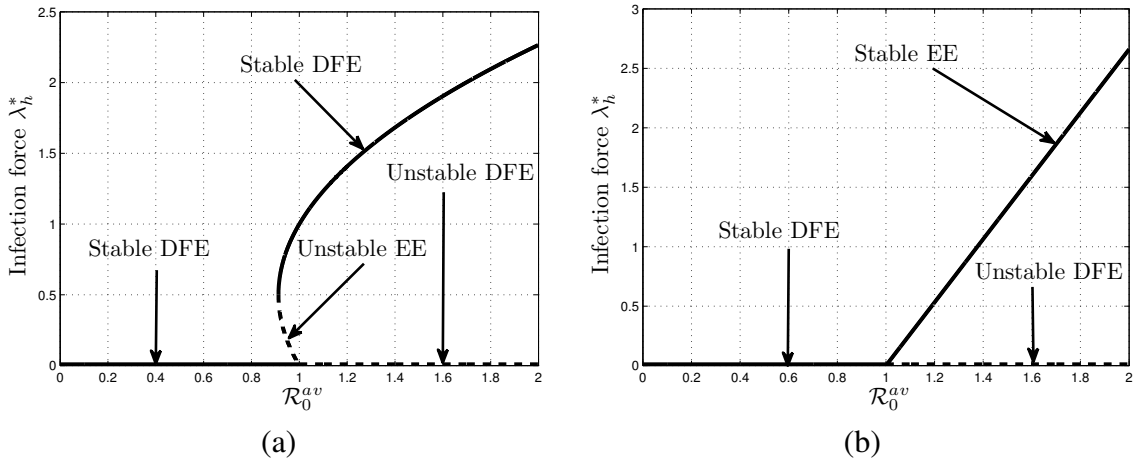

Figure 3. Bifurcation diagrams for system (6). (a) $\beta_a = 0.573$ and $\theta = 0.4868$ (so that $\mathcal{A} = 0.000040162132\ u_5^2 v_3 > 0$) and (b) $\beta_a = 0.573$ and $\theta = 0.04868$ (so that $\mathcal{A} = -0.000047658774\ u_5^2 v_3 < 0$). EEP denotes the endemic equilibrium point. All other parameter values are as in Table 2.

Figure 4 plots the phase portrait of system (6) when $\beta_h = 0.83345$ and $\beta_a = 0.573$ (so that $\mathcal{R}_0 = 1.226360785 > 1$). It illustrates the fact that the trajectories of system (6) converge to the endemic equilibrium point E^*. This means that *NmA* persists within the community and the disease is uncontrollable.

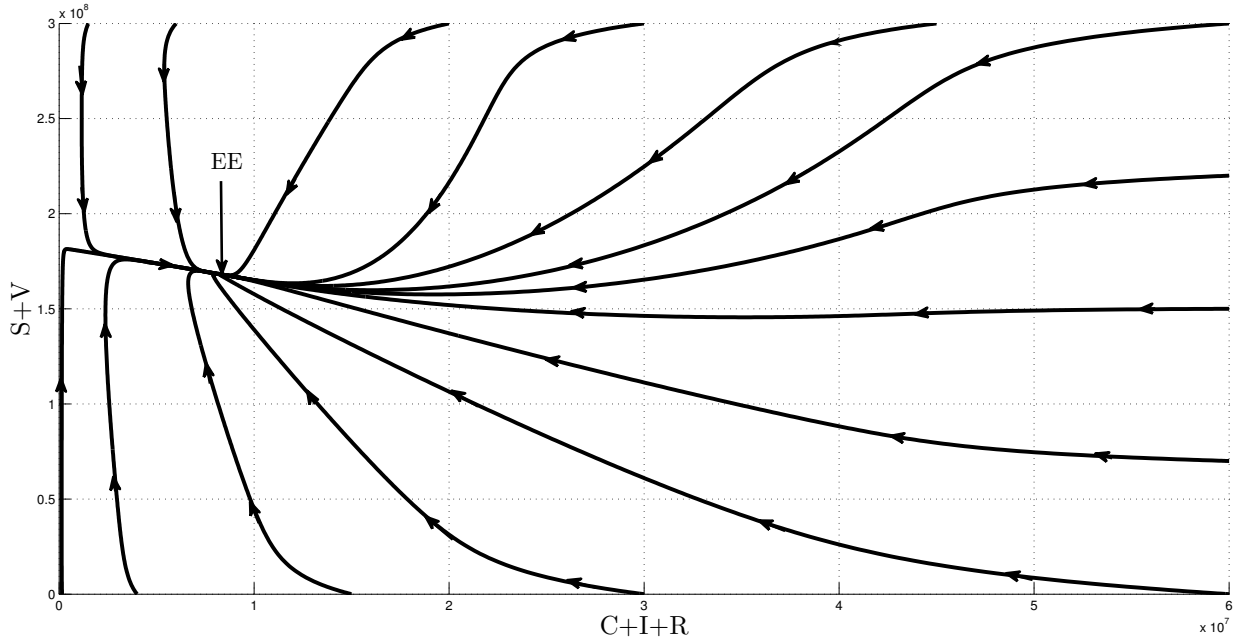

Figure 4. Asymptotic (global) stability of the unique EE when $\mathcal{R}_0 > 1$. Here, $\beta_h = 0.83345$ and $\beta_a = 0.573$ (so that $\mathcal{R}_0 = 1.226360785 > 1$). All other parameter values are as in Table 2.

4. Impact of desert aerosols and vaccine on the time evolution of *NmA*

In this section, we investigate the role of desert aerosols and vaccine on the dynamical transmission of *NmA*. To allow an easy assessment, we start by studying the corresponding sub-model without desert aerosols. Obviously, in the absence of desert aerosols, $(\beta_a = 0)$, our initial model (5) reduces to the following sub-model,

$$\begin{cases} \dot{S} = \Lambda + \omega V - (\theta + \mu + \lambda_h)S + \varphi R, \\ \dot{V} = \theta S - (\omega + \mu + (1-\nu)\lambda_h)\, V, \\ \dot{C} = (S + (1-\nu)V)\, \lambda_h - (\mu + \alpha + \gamma)\, C, \\ \dot{I} = \gamma C - (\mu + d + \delta)I, \\ \dot{R} = \delta I + \alpha C - (\varphi + \mu)R. \end{cases} \tag{32}$$

This aerosol-free model is exactly the same as the one in Agusto and Leite (2019), which in turn is a simplification of the model in Djatcha Yaleu et al. (2017) if newborns are not vaccinated against *NmA* at birth. The interested readers are referred to the latter two works for their in-depth analysis. The system (6) and system (32) have the same DFE and the basic reproduction number $\mathcal{R}_0^{(a,f)}$ of (32) is obtained by letting $\beta_a = 0$ in the expression of $\mathcal{R}_0^{av}$ given by (14). That is:

$$\mathcal{R}_0^{(a,f)} = \frac{\Sigma^0 \left(S^0 + (1-\nu)V^0\right)(\varepsilon D_2 + \gamma)}{D_1 D_2}. \tag{33}$$

Although the full model (6) with aerosol and the aerosol-free sub-model (32) have similar theoretical results as far as the bifurcation analysis is concerned. Below, the influence of desert aerosol is assessed in terms of its impact on the disease outbreak and and level of endemicity.

4.1. Detrimental impact of desert aerosols on *NmA*

We start the assessment of the role of desert aerosol on the transmission of *NmA* by comparing the basic reproduction numbers of the models in the presence of desert aerosols and its aerosol-free sub-model. Practically, the basic reproduction for an epidemic such as*NmA* measures its ability to invade the human population. In order to achieve our goal, we compute the ratio:

$$\frac{\mathcal{R}_0^{(a,f)}}{\mathcal{R}_0^{av}} = \frac{\left(S^0 + (1-\nu)V^0\right)(\varepsilon D_2 + \gamma)}{D_3\left(\varepsilon D_2 + \gamma\right) + D_1 D_4}.$$

Since $D_3 = \left((1-p)\lambda_a^0 + 1\right) S^0 + \left((1-q)\lambda_a^0 + 1\right)(1-\nu)V^0$, one has $\left(S^0 + (1-\nu)V^0\right) < D_3$, and consequently $\left(S^0 + (1-\nu)V^0\right)(\varepsilon D_2 + \gamma) < D_3\left(\varepsilon D_2 + \gamma\right)$, leading to

$$\mathcal{R}_0^{(a,f)} < \mathcal{R}_0^{av}. \tag{34}$$

The relation (34) suggests that the inhalation of aerosols dust is detrimental to the transmission of *NmA* by increasing its ability to break and invade the population. Moreover, neglecting the effects of desert aerosols might lead to an underestimate of the basic reproduction number and potentially distort the efforts undertaken to eliminate *NmA*.

Figure 5 plots the basic reproduction numbers $\mathcal{R}_0^{(a,f)}$ and $\mathcal{R}_0^{av}$ as a function of β_h for two different and fixed values of β_a. It shows that $\mathcal{R}_0^{(a,f)}$ and $\mathcal{R}_0^{av}$ are increasing functions of β_h. In fact, their analytically expressions show that they are increasing linear functions of β_h.

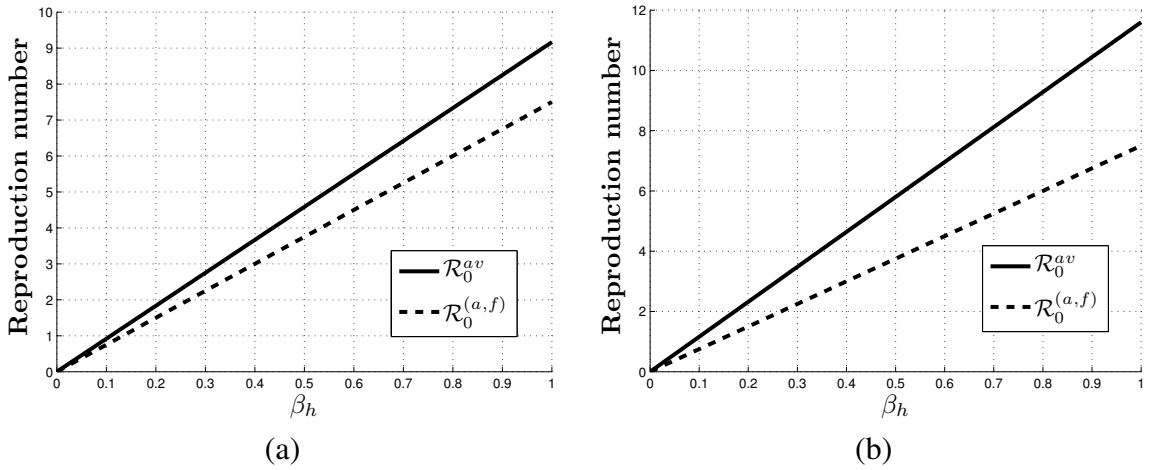

Figure 5. Comparison between $\mathcal{R}_0^{av}$ and $\mathcal{R}_0^{(a,f)}$ for fixed values of β_a. They are plotted as the function of β_h: (a) $\beta_a = 0.3$ and (b) $\beta_a = 0.983$. All other parameter values are as in Table 2.

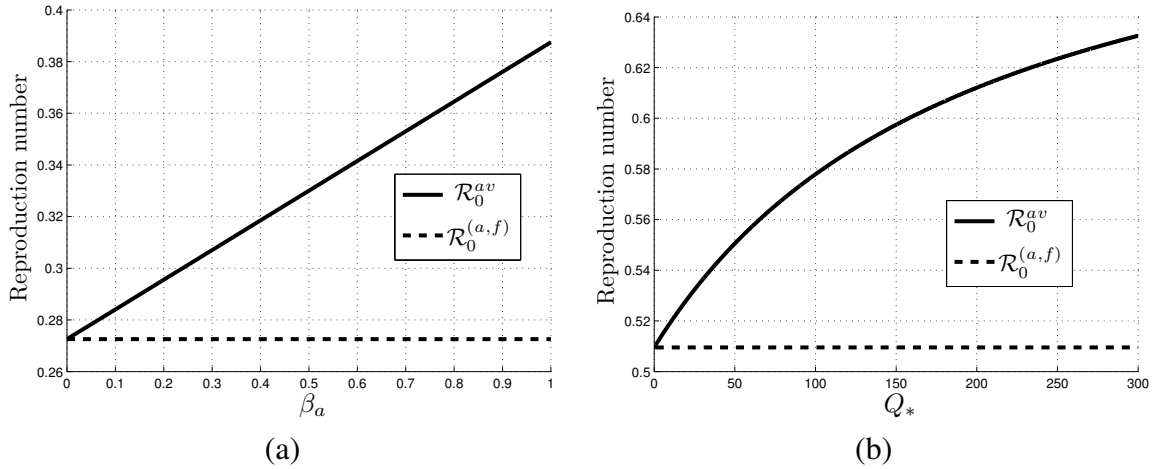

Figure 6. Comparison between $\mathcal{R}_0^{av}$ and $\mathcal{R}_0^{(a,f)}$ for fixed values of β_h. They are plotted against β_a and Q_*. (a) $\beta_h = 0.43$. (b) $\beta_h = 0.43$ and $\beta_a = 0.53$. All other parameter values are as in Table 2.

Now, we investigate the dependence of the reproduction number $\mathcal{R}_0^{av}$ with respect to β_a in the one hand, and to Q_* in the other hand. The partial derivatives of $\mathcal{R}_0^{av}$ with respect to β_a and Q_* are respectively,

$$\frac{\partial \mathcal{R}_0^{av}}{\partial \beta_a} = \frac{\Sigma^0 A^0 \left\{(\varepsilon D_2 + \gamma)\left((1-p)S^0 + (1-q)k_7 V^0\right) + D_1\left(pS^0 + qk_7 V^0\right)\right\}}{(A^0 + H)D_1 D_2}, \tag{35}$$

and

$$\frac{\partial \mathcal{R}_0^{av}}{\partial Q_*} = \frac{\Sigma^0 \beta_a \mu_a H \left\{(\varepsilon D_2 + \gamma)\left((1-p)S^0 + (1-q)k_7 V^0\right) + D_1\left(pS^0 + qk_7 V^0\right)\right\}}{\left(Q_* + \mu_a H\right)^2 D_1 D_2}. \tag{36}$$

Thus, $\mathcal{R}_0^{av}$ is an increasing function of β_a and Q_*, respectively.

Relations (35) and (36) show that a high contact rate with desert aerosol or a large value of aerosol production might lead to a very large value of the basic reproduction number consequently have a considerable detrimental impact on the spreading of *NmA*. This is illustrated in Figure 6. Looking at $\mathcal{R}_0^{av}$ as a function of the two variables β_h and β_a (ie. $\mathcal{R}_0^{av} = \mathcal{R}_0^{av}(\beta_h, \beta_a)$) and using parameter values in Table 2, we illustrate numerically in Figure 7 that an increase in both the inhalation rate of desert aerosols β_a and the *NmA* transmission rate β_h results to an increase in $\mathcal{R}_0^{av}$.

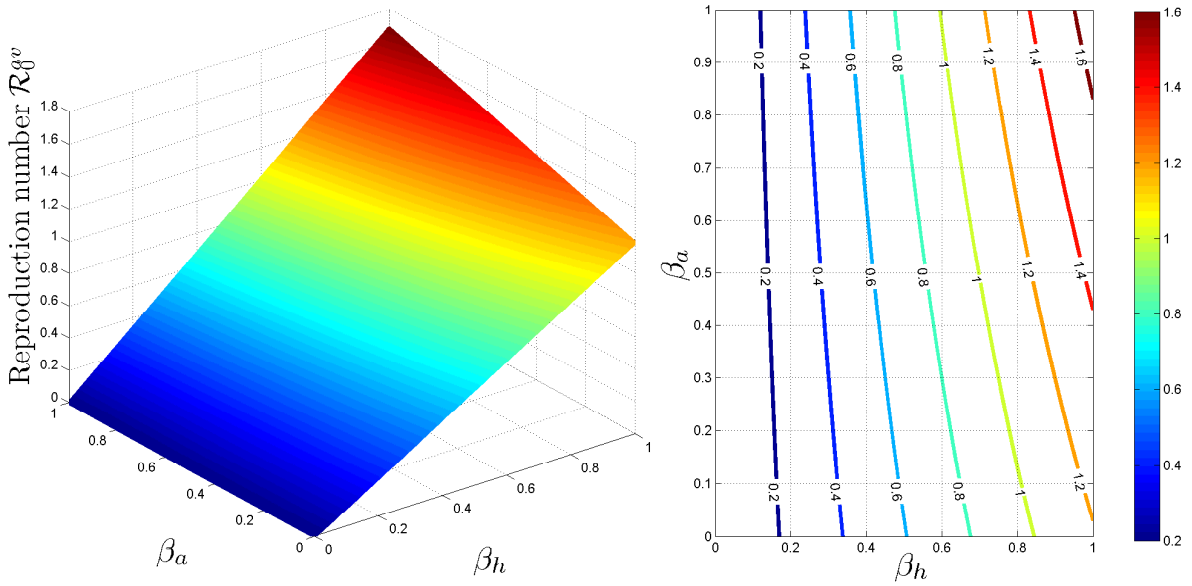

Figure 7. Level curves of the reproduction number $\mathcal{R}_0^{av}$ showing the simultaneous effects of β_h and β_a. All other parameter values are as in Table 2.

We close up this investigation by evaluating the effects of desert aerosol on the level of the endemicity of *NmA*. The simpler way of doing this is to study the behavior of the unique endemic equilibrium ($\mathcal{R}_0^{av} > 1$) as a function of the irritation rate β_a. Precisely, we study the behavior of the infected component $I^{**}(\beta_a)$ as a function of β_a. Remember that

$$I^{**} = I^{**}(\beta_a) = \frac{e_{15}(\beta_a)(\lambda_h^{**}(\beta_a))^2 + e_{16}(\beta_a,)\lambda_h^{**}(\beta_a)}{e_{10}(\beta_a)(\lambda_h^{**}(\beta_a))^2 + e_{11}(\beta_a)\lambda_h^{**}(\beta_a) + e_{12}(\beta_a)},$$

with

$$\lambda_h^{**}(\beta_a) = \frac{-e_{20}(\beta_a) + \sqrt{(e_{20}(\beta_a))^2 - 4e_{21}(\beta_a)e_{19}(\beta_a)}}{2e_{19}(\beta_a)}.$$

Now, from Equation (26), the partial derivative of I^{**} with respect to β_a satisfies

$$\frac{\partial I^{**}}{\partial \beta_a} = \frac{K_0 + K_1(\lambda_h^{**})^4 + K_2(\lambda_h^{**})^3 + K_3(\lambda_h^{**})^2}{\left(e_{10}(\lambda_h^{**})^2 + e_{11}\lambda_h^{**} + e_{12}\right)^2}, \tag{37}$$

where

$$K_0 = \left((\lambda_h^{**})^2 \frac{\partial e_{15}}{\partial \beta_a} + 2e_{15}\lambda_h^{**}\frac{\partial \lambda_h^{**}}{\partial \beta_a} + \lambda_h^{**}\frac{\partial e_{16}}{\partial \beta_a} + e_{16}\frac{\partial \lambda_h^{**}}{\partial \beta_a} \right) e_{12},$$

$$\begin{aligned}
K_1 =& \; A^0 {k_7}^2 p\mu\,\Lambda\,\left(1+\beta_a A^0\right)^2 (\mu+\varphi)\,(\mu+\varphi+\alpha)\,(\mu+\alpha+\,\gamma)\,(\mu+d+\delta)\,/(A^0+H),\\
K_2 =& \; A^0 k_7 \mu\,\Lambda\,(\mu+\varphi)\,(\mu+\alpha+\,\gamma)\,(\mu+d+\delta)\left(1+\beta_a A^0\right)\big[k_7\big(\gamma\mu+p\alpha\,\varphi+\theta\,p\alpha\\
&+\theta\,p\varphi+\theta\,q\alpha+\theta\,q\varphi+\,\gamma\varphi+\mu\,p\varphi+\mu\,\theta\,q+\mu\,p\alpha+\mu\,\theta\,p+A^0\mu\,\beta_a p\varphi+A^0 p\beta_a\alpha\,\varphi\\
&+(p-q)\beta_a A^0\theta\,(\mu+\alpha+\varphi)+A^0\,\gamma\beta_a\mu+A^0\,\gamma\varphi\,\beta_a+A^0 p\beta_a\mu^2+A^0\mu\,\beta_a p\alpha+\mu^2 p\big)\\
&+2\,\mu\,p\omega+2\,\mu\,\alpha\,p+2\,p\omega\,\alpha+2\,p\omega\,\varphi+2\,\mu\,\varphi\,p+2\,\mu^2 p\big]/(A^0+H),\\
K_3 =& \; A^0\mu\,(\mu+\varphi)\,\Lambda\left(\mu^2+\mu\,\alpha+k_7(\mu^2+\mu\,\varphi+\mu\,\theta+\mu\,\alpha+\theta\,\varphi+\theta\,\alpha+\varphi\,\alpha)+\mu\,\varphi+\mu\,\omega\right.\\
&\left.+\,\omega\,\alpha+\omega\,\varphi\right)(k_7\theta\,q+\mu\,p+p\omega)\,D_1D_2/(A^0+H)+\mu\,\Lambda\,(1-\nu)^2\,\big[\,\left(1+\lambda_a^0\right)(\mu+\varphi)\,\gamma\\
&+(\mu^2+\mu\alpha+\mu\varphi+\alpha\varphi)\lambda_a^0 p+(p-q)\lambda_a^0\theta(\mu+\alpha+\varphi)\big]\,\left(1+\lambda_a^0\right)^2(\mu+\varphi)\,D_1D_2(\partial\lambda_h^{**}/\partial\beta_a).
\end{aligned}$$

Analytically, it is very difficult to prove that $\partial I^{**}/\partial\beta_a > 0$. Alternatively, we illustrate it numerically in Figure 8 which shows that I^{**} and C^{**} are increasing functions of β_a. Thus, we have established the following result.

Theorem 4.1.

The infected components $I^{**} = I^{**}(\beta_a)$ and $C^{**} = I^{**}(\beta_a)$ of the endemic equilibrium point are strictly monotonic increasing functions on the interval $0 \leq \beta_a < +\infty$.

The relevance of Theorem 4.1 is that it suggests a clear answer to the research question which has motivated this work, by highlighting the detrimental effect of the desert aerosols in the transmission of meningococcal meningitis. To add more evidence, Figure 8 presents the time series of infected individuals for three different values of β_a when β_h is fixed to $\beta_h = 0.983345$ (so that $\mathcal{R}_0^{(a,f)} > 1$). From this figure, it clearly appears that as β_a increases, the number of carriers and infectious individuals increases. This shows the detrimental impact of aerosols at every time step of the evolution of *NmA*.

4.2. Favorable impact of vaccine

Now, we assess the effect of vaccination on system (6). To do this, we consider a control strategy consisting in vaccinating the susceptible individuals. Suppose that initially (i.e., at $t = 0$), a proportion θ of susceptible individuals is vaccinated with an imperfect vaccine. The basic reproduction number of corresponding sub-model of system (6) in the absence of vaccination is obtained when $\theta = 0$ and reads as

$$\mathcal{R}_0 = \frac{\Sigma^0 N^0\left\{((1-p)\lambda_a^0+1)\,(\varepsilon D_2+\gamma)+p\lambda_a^0 D_1\right\}}{D_1D_2}. \tag{38}$$

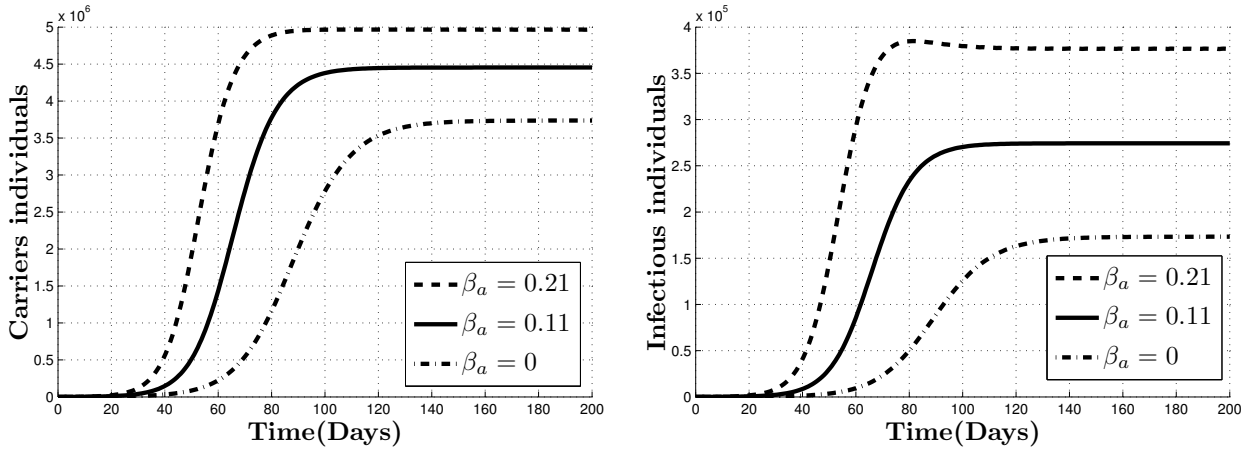

Figure 8. Time series of infected individuals for three different values of β_a when $\beta_h = 0.983345$ (so that $\mathcal{R}_0^{(a,f)} > 1$): (a) carriers C and (b) infectious I. All other parameter values are as in Table 2.

The basic reproduction $\mathcal{R}_0^{av}$ of the full system (6) and its vaccination-free sub-model counterpart $\mathcal{R}_0$ are linked by the following relation:

$$\mathcal{R}_0^{av} = \frac{D_3\left(\varepsilon D_2 + \gamma\right) + D_1 D_4}{N^0\left\{\left((1-p)\lambda_a^0 + 1\right)\left(\varepsilon D_2 + \gamma\right) + p\lambda_a^0 D_1\right\}}\mathcal{R}_0. \tag{39}$$

From (39), one clearly sees that $\mathcal{R}_0^{av} < \mathcal{R}_0$, which shows that vaccination reduces the basic reproduction number, and potentially impedes the *NmA* to break out in a severe manner. The constraint $\mathcal{R}_0^{av} < 1$ is necessary (but not always sufficient) for the elimination of *NmA*, and defines implicitly the critical vaccination threshold rate θ_c given by:

$$\theta_c = \frac{\left\{\left((1-p)\lambda_a^0 + 1\right)\left(\varepsilon D_2 + \gamma\right) + p\lambda_a^0 D_1\right\}\left(\mu + \omega\right)\left(\mathcal{R}_0 - 1\right)}{\left\{\left((1-p)\lambda_a^0 + 1\right)\left(\varepsilon D_2 + \gamma\right) + p\lambda_a^0 D_1\right\} - \mathcal{R}_0 k_7\left\{\left((1-q)\lambda_a^0 + 1\right)\left(\varepsilon D_2 + \gamma\right) + q\lambda_a^0 D_1\right\}}. \tag{40}$$

If there were no backward bifurcation phenomenon, the vaccination rate satisfying $\theta > \theta_c$ will have been necessary and sufficient to ensure the elimination of *NmA*. One should notice that even in this case, the vaccination at the critical rate θ_c which guaranties the so called herd immunity (Scherer and McLean (2002); Farrington (2003)), will not instantly lead to the disease elimination, because the human immunity requires time to build up (McLeod Griffiss (1995)). Unfortunately, for the current work, the phenomenon of backward bifurcation is present and complicates the control of the disease by requiring more implementable efforts to bring $\mathcal{R}_0^{av}$ below the threshold value ξ_1. This additional constraint, coupled to $\mathcal{R}_0^{av} < 1$ is (thanks to Theorem 3.2) necessary and sufficient to eliminate *NmA*. Note that the constraint $\mathcal{R}_0^{av} \leq \xi_1$ will be easily achieved if by chance the threshold value ξ_1 is as large as possible, and close to 1 from the left. The latter constraint (imposed by the existence of backward bifurcation phenomenon) enforces a second vaccination threshold rate θ_c^e that must be reached for *NmA* elimination. The explicit value of θ_c^e seems impossible to be derived due to the fact that vaccination is not 100% efficient. Alternatively, it is rather possible to compute the threshold effectiveness rate of vaccination ν^c so that $\nu \geq \nu^c$ is equivalent to $\mathcal{R}_0^{av} \leq \xi_1$. The

said threshold reads:

$$\nu^c = 1 - \frac{\{((1-p)\lambda_a^0 + 1)(\varepsilon D_2 + \gamma) + p\lambda_a^0 D_1\}\left(1 - \mathcal{R}_0\right)}{\{((1-q)\lambda_a^0 + 1)(\varepsilon D_2 + \gamma) + q\lambda_a^0 D_1\}\mathcal{R}_0}. \tag{41}$$

Finally, *NmA* can be eliminated in the population when people are vaccinated at the rate θ above θ_c, using a vaccine whose efficiency rate ν exceeds ν^c.

The above theoretical investigations are now numerically ascertained. In this regard, we assume that a vaccine with 80.5% ($\nu = 0.805$) efficacy is used, and choose $\beta_h = 0.4334$ and $\beta_a = 0.673$. Taking the remaining parameters values as in Table 2, the threshold efficacy rate necessary for the elimination of *NmA* is $\theta_c = 0.2697$. In order to illustrate that the constraint $\theta > \theta_c$ is not sufficient to eliminate *NmA*, we choose values of θ around θ_c in the following three scenarios:
(i) $\theta = 0.2667$ (so that $\mathcal{R}_0^{av} = 1.0022$ and $\theta < \theta_c$),
(ii) $\theta = 0.2697$ (so that $\mathcal{R}_0^{av} = 1.0000$ and $\theta = \theta_c$),
(iii) $\theta = 0.2717$ (so that $\mathcal{R}_0^{av} = 0.9986$ and $\theta > \theta_c$).

Since in either case, $\mathcal{R}_0^{av} \geq 1$, *NmA* cannot be eliminated. This is reinforced by Figure 9, which shows that all infected individuals remain positive for all time.

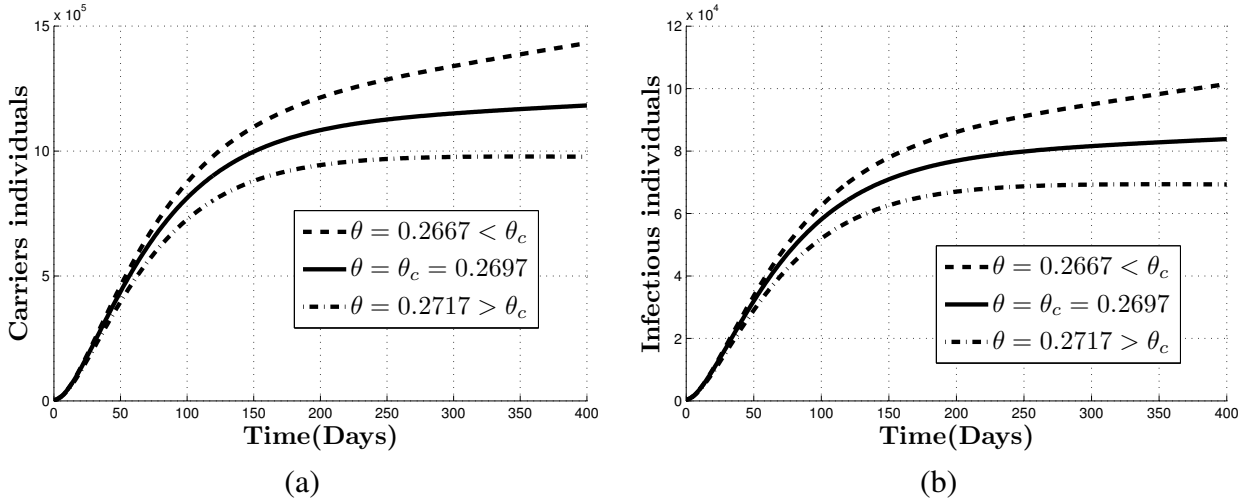

Figure 9. Infected individuals for three different values of proportion of susceptible population vaccinated when $\beta_h = 0.4334$ and $\beta_a = 0.673$ (so that $\theta_c = 0.2697$): (a) carriers C and (b) infectious I. All other parameter values are as in Table 2.

We have just shown that vaccination alone in not sufficient to eliminate *NmA* in the population. Nevertheless, vaccination with efficacy above the control threshold ν^c is enough. Therefore, we assume that 0.85% ($\theta = 0.0085$) of susceptible individuals are vaccinated against *NmA* and we take $\beta_h = 0.1028$ and $\beta_a = 0.6930$. Using the parameter values in Table 2, we obtain $\nu^c = 0.9177$. Thus, to illustrate that the constraint $\nu > \nu^c$ is sufficient to eliminate *NmA*, we choose three values of ν close to ν^c. The following three cases are considered:
(a) $\nu = 0.1801 < \nu^c$ (so that $\mathcal{R}_0^{av} = 0.8822$) and $\xi_1 = 0.5147$),

(b) $\nu = 0.1897 < \nu^c$ (so that $\mathcal{R}_0^{av} = 0.8794$ and $\xi_1 = 0.5159$),
(c) $\nu = 0.9877 > \nu^c$ (so that $\mathcal{R}_0^{av} = 0.6472$ and $\xi_1 = 0.6943$).

These three cases are illustrated in Figure 10, where it is clear that *NmA* will be eliminated only when $\nu > \nu^c$. Theoretically, the elimination scenario in (c) corresponds to the situation where $\mathcal{R}_0^{av} < \xi_1 < 1$ (because $\mathcal{R}_0^{av} = 0.6472 < \xi_1 = 0.6943$) as demonstrated earlier in Theorem 3.2.

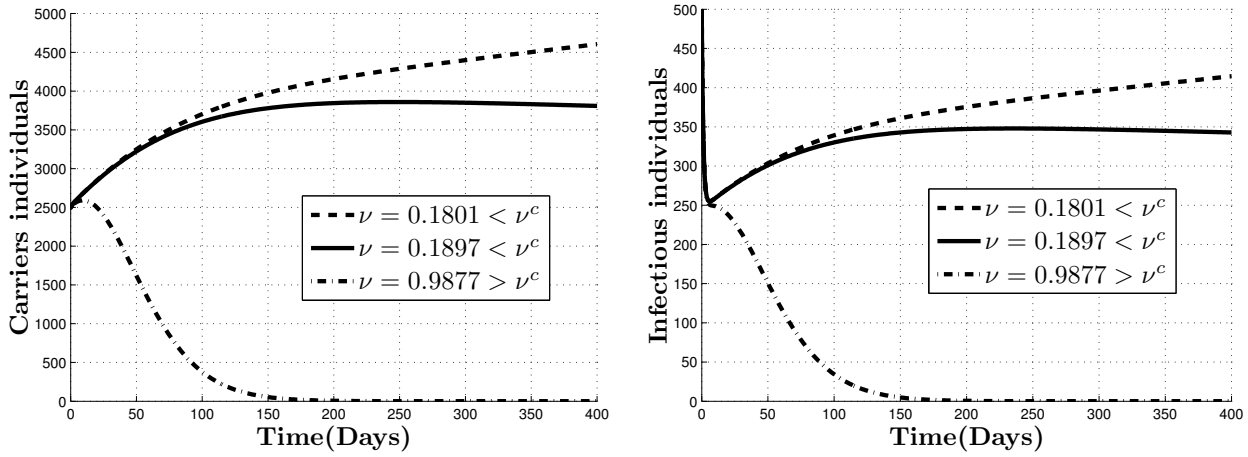

Figure 10. Infected individuals for three different values of proportion of susceptible population vaccinated when $\beta_h = 0.1028$ and $\beta_a = 0.6930$ (so that $\nu^c = 0.9177$): (a) carriers C and (b) infectious I. All other parameter values are as in Table 2.

5. Discussion and Conclusion

5.1. Discussion

The model was built in such a way that its basic reproduction number is greater than its counterpart in the absence of aerosols. This finding suggests that, ignoring the influence of aerosol dust may under-estimate the ability of *NmA* to break out and invade the population and possibly distort the *NmA* control strategies. The detrimental impact of desert aerosols on the long run dynamics of *NmA* was shown by proving that at the endemic level of *NmA*, the number of infected individuals increases when the aerosol dust inhalation rate increases. More importantly, our model suggests that the successful elimination of *NmA* can be achieved by vaccinating, with a vaccine that assumes a sufficiently high efficacy. This was shown by exhibiting a threshold value for vaccine efficacy, above which the vaccine efficacy should lie in order to eliminate *NmA*.

5.2. Conclusion

In this paper, we have assessed the influences of desert aerosols on the dynamical transmission of *NmA* in a human population where an imperfect vaccine is used to prevent the disease propagation.

The assessment was done through the formulation of a mathematical model which accounted for the fast and slow progressions of *NmA* due to the inhalation of aerosol dust that weakens the nasopharyngeal mucosa of afflicted individuals. Our theoretical and numerical findings and other contributions can be summarized as follows: (a) We have proved the existence, boundedness and positivity of a unique global solution of any initial problem of the model. (b) We have computed the basic reproduction number and used to study the existence and types of equilibria and their stability properties. (c) We have exhibited an additional threshold such that: (i) the disease-free equilibrium is globally asymptotically stable whenever that additional threshold is between the basic reproduction number and 1, (ii) the model undergoes the backward and forward bifurcations. (d) We have shown that there exists a unique locally asymptotically stable endemic equilibrium whenever the basic reproduction number is greater than one, but close to 1. (e) We have plotted the graphs and diagrams to illustrate backward and forward bifurcations exhibited by our model and the asymptotic (global) of equilibria, as well as the detrimental impact of aerosol dust due to its the inhalation.

Our findings have informed the possible extensions of the current work on which we are already working. They include: (1) The explicit incorporation of seasonality by considering time-periodic parameters for the equation for aerosols. (2) Introducing the diffusion and transport of aerosol dust by wind by considering a reaction-diffusion-convection model. (3) Incorporating some control strategies such as watering the routes and educating people to avoid huge gatherings.

Acknowledgment:

The authors are very grateful to the Editor-in-Chief and the anonymous reviewers for their comments and suggestions which helped to improve the quality of this work.

REFERENCES

Agier, L., Deroubaix, A., Martiny, N., Yaka, P., Djibo, A. and Broutin, H. (2012). Seasonality of meningitis in Africa and climate forcing: Aerosols stand out, Journal of the Royal Society Interface, Vol. 10, No. 79, pp. 20120814.

Agusto, F. B. and Leite, M. (2019). Optimal control and cost-effective analysis of the 2017 meningitis outbreak in Nigeria, Infectious Disease Modelling, Vol. 4, pp. 161-187.

Alonso, J. M., Bertherat, E., Perea, W., Borrow, R., Chanteau, S., Cohet, C., Dodet B., Greenwood B., LaForce F.M., Muros-Le Rouzic E., Teyssou R., Ouédraogo-Traoré R. and Sow, I. (2006). From genomics to surveillance, prevention and control: New challenges for the African meningitis belt, Bulletin de la Societe de pathologie exotique, Vol. 99, No. 5, pp. 404-408.

Anderson, R.-M. and May, R.-M. (1992). *Infectious Disease of Humans, Dynamical and Control*, Oxford: Oxford University Press.

Asamoah, J., Nyabadza, F., Seidu, B., Chand, M. and Dutta, H. (2018). Mathematical modelling of bacterial meningitis transmission dynamics with control measures, Computational and Mathematical Methods in Medicine, Vol. 2018, pp. 2657461.

Bah, O.A., Lam, M., Bah, A. and Bowong, S. (2019). Theoretical assessment of the impact of desert aerosols on the dynamical transmission of meningitidis serogroup A, International Journal of Biomathematics, Vol. 12, pp. 1950060.

Bani-Yaghoub, M., Gautam, R., Shuai, Z., van den Driessche, P. and Ivanek, R. (2012). Reproduction numbers for infections with free-living pathogens growing in the environment, Journal of Biological Dynamics, Vol. 6, pp. 923-940.

Bingen E. (2001). *Méningites bactériennes communautaires*, Paris: Elsevier Masson.

Blyuss, K.B. (2016). Mathematical modelling of the dynamics of meningococcal meningitis in Africa, UK Success Stories in Industrial Mathematics, pp. 221-226.

Boisier, P., Nicolas, P., Djibo, S., Taha, M. K., Jeanne, I., Maínassara, H. B., Tenebray, B., Kairo, K. K., Giorgini, D. and Chanteau, S. (2007). Meningococcal meningitis: unprecedented incidence of serogroup X-related cases in 2006 in Niger, Clinical infectious diseases: Sn official publication of the Infectious Diseases Society of America, Vol. 44, No. 5, pp. 657-663.

Bornaa, C.S., Makinde, O.D. and Seini, I.Y. (2015). Eco-epidemiological model and optimal control of disease transmission between humans and animals, Commun. Math. Biol. Neurosci, Vol. 2015, Article-ID 26.

Bou Karam, D., Flamant, C., Tulet, P., Chaboureau, J.-P., Dabas, A. and Todd, M.C. (2009). Estimate of Sahelian dust emissions in the intertropical discontinuity region of the West African Monsoon, J. Geophys. Res. Vol. 114, No. D13, pp. D13106.

Bowong, S., Mountaga, L., Bah, A., Tewa, J.J. and Kurths, J. (2016). Parameter and state estimation in a Neisseria meningitidis model: A study case of Niger, Chaos (Woodbury, N.Y.), Vol. 26, No. 12, 123115.

Brauer, F. (2004). Backward bifurcations in simple vaccination models, Journal of Mathematical Analysis and Applications, Vol. 298, No. 2, pp. 418-431.

Broome, C.V., Rugh, M.A., Yada, A.A., Giat, L., Giat, H., Zeltner, J.M., Sanborn, W.R. and Fraser, D.W. (1983). Epidemic group C meningococcal meningitis in Upper Volta, 1979, Bulletin of the World Health Organization, Vol. 61, No. 2, pp. 325-330.

Capasso, V. (1993). *Mathematical Structures of Epidemic Systems* (Vol. 88), Berlin: Springer.

Carr, J. (1981). *Applications Centre Manifold Theory*, Springer-Verlag, New York.

Cartwright, K. (1995). Meningococcal carriage and disease, in: Cartwright, K. (Ed.), *Meningococcal Disease*, Wiley and Sons, Chichester, UK, pp. 113-146.

Castillo-Chavez, C. and Song, B. (2004). Dynamical models of tuberculosis and their applications, Math. Biosci. Eng., Vol. 1, pp. 361-404.

Centers for Disease Control and Prevention. (2011). Updated recommendations for use of meningococcal conjugate vaccines advisory committee on immunization practices (acip), 2010. MMWR. Morbidity and Mortality Weekly Report, Vol. 60, No. 3, pp. 72.

Coen, P.G., Cartwright, K. and Stuart, J. (2000). Mathematical modelling of infection and disease due to Neisseria meningitidis and Neisseria lactamica, International Journal of Epidemiology, Vol. 29, No. 1, pp. 180-188.

De Longueville, F., Henry, S. and Ozer, P. (2014). Première évaluation des impacts des poussières

désertiques sur la santé des enfants en Afrique de l'Ouest : étude de cas dans le Bénin septentrional, XXVIIe colloque de l'Association internationale de climatologie, pp. 536-542.

Decosas, J. and Koama, J.B. (2002). Chronicle of an outbreak foretold: Meningococcal meningitis W135 in Burkina Faso, The Lancet Infectious Diseases, Vol. 2, No. 12, pp. 763-765.

Deghmane, A.-E., Taha, M.-K. (2010). Physiopathologie des infections invasives à méningocoque, Médecine Thérapeutique Pédiatrie, Vol. 13, pp. 117-122.

Diekmann, O., Heesterbeek, J. A. and Metz, J. A. (1990). On the definition and the computation of the basic reproduction ratio R0 in models for infectious diseases in heterogeneous populations, Journal of Mathematical Biology, Vol. 28, No. 4, pp. 365-382.

Diekmann, O., Heesterbeek, J.A.P. and Roberts, M.G. (2010). The construction of next-generation matrices for the compartmental epidemic models of disease transmission, J. R. Soc. Interface, Vol. 7, pp. 873-885.

Djatcha Yaleu, G., Bowong, S., Houpa Danga, E. and Kurths, J. (2017). Mathematical analysis of the dynamical transmission of Neisseria meningitidis serogroup A, International Journal of Computer Mathematics, Vol. 94, No. 12, pp. 2409-2434.

Dushoff, J., Huang, W. and Castillo-Chavez, C. (1998). Backwards bifurcations and catastrophe in simple models of fatal diseases, Journal of Mathematical Biology, Vol. 36, No. 3, pp. 227-248.

Farrington, C. (2003). On vaccine efficacy and reproduction numbers, Math. Biosci., Vol. 185, pp. 89-101.

Gandon, S., Mackinnon, M., Nee, S. and Read, A. (2003). Imperfect vaccination: Some epidemiological and evolutionary consequences, Proceedings of the Royal Society of London, Series B: Biological Sciences, Vol. 270, No. 1520, pp. 1129-1136.

Garba, S.M., Gumel, A.B. and Bakar, M.R.A. (2008). Backward bifurcations in dengue transmission dynamics, Mathematical Biosciences, Vol. 215, No. 1, pp. 11-25.

Greenwood B. (1999). Manson Lecture. Meningococcal meningitis in Africa, Transactions of the Royal Society of Tropical Medicine and Hygiene, Vol. 93, No. 4, pp. 341-353.

Harrison, L.H., Trotter, C.L. and Ramsay, M.E. (2009). Global epidemiology of meningococcal disease, Vaccine, Vol. 27, pp. B51-B63.

Hepkema, H., Pouwels, K.B., van der Ende, A., Westra, T.A. and Postma, M.J. (2013). Meningococcal serogroup A, C, W135 and Y conjugated vaccine: A cost-effectiveness analysis in the Netherlands, PloS One, Vol. 8, No. 5, e65036.

Hethcote, H.W. (2000). The mathematics of infectious diseases, SIAM Review, Vol. 42, No. 4, pp. 599-653.

Irving, T.J., Blyuss, K.B., Colijn, C. and Trotter, C.L. (2012). Modelling meningococcal meningitis in the African meningitis belt, Epidemiology and Infection, Vol. 140, No. 5, pp. 897-905.

Kamgang, J-C. and Sallet, G. (2008) Computation of threshold conditions for epidemiological models and global stability of the disease-free equilibrium (DFE), Math. Biosci., Vol. 213, pp. 1-12.

Kimaro, M. A., Massawe, E. S. and Makinde, D. O. (2015). Modelling the optimal control of transmission dynamics of mycobacterium ulceran infection, Open Journal of Epidemiology, Vol. 5, No. 4, pp. 229.

Lapeyssonnie, L.(1963). La méningite cérébrospinale en Afrique, Bull Organ Mond Santé , Vol. 28, pp. 3-114

Laurent, B., Marticorena, B., Bergametti, G., Léon, J. F. and Mahowald, N. M. (2008). Modeling mineral dust emissions from the Sahara desert using new surface properties and soil database, Journal of Geophysical Research: Atmospheres, Vol. 113(D14).

Leimkugel, J., Hodgson, A., Forgor, A. A., Pfléger, V., Dangy, J. P., Smith, T., Achtman, M., Gagneux, S. and Pluschke, G. (2007). Clonal waves of Neisseria colonisation and disease in the African meningitis belt: Eight-year longitudinal study in northern Ghana, PLoS Medicine, Vol. 4, No. 3, pp. e101.

Leimkugel, J., Racloz, V., da Silva, L. J. and Pluschke, G. (2009). Global review of meningococcal disease. A shifting etiology, African Journal of Bacteriology Research, Vol. 1, No. 1, pp. 006-018.

Martcheva, M. and Crispino-O'Connell, G. (2003). The transmission of meningococcal infection: A mathematical study, Journal of Mathematical Analysis and Applications, Vol. 283, pp. 251-275.

Martiny, N. and Chiapello, I. (2013). Assessments for the impact of mineral dust on the meningitis incidence in West Africa, Atmospheric Environment, Vol. 70, pp. 245-253.

McLeod Griffiss, J. (1995). Mechanisms of host immunity, in: Cartwright, K. (Ed.), *Meningococcal Disease*, Wiley and Sons, Chichester, UK , pp. 35-70.

Molesworth, A. M., Thomson, M. C., Connor, S. J., Cresswell, M. P., Morse, A. P., Shears, P., Hart, C. A. and Cuevas, L. E. (2002). Where is the meningitis belt? Defining an area at risk of epidemic meningitis in Africa, Transactions of the Royal Society of Tropical Medicine and Hygiene, Vol. 96, No. 3, pp. 242-249.

Moore, P.S. (1992). Meningococcal meningitis in sub-Saharan Africa: A model for the epidemic process, Clinical Infectious Diseases: An Official Publication of the Infectious Diseases Society of America, Vol. 14, No. 2, pp. 515-525.

Mueller, J-E. and Gessner, B-D. (2010). A hypothetical explanatory model for meningococcal meningitis in the African meningitis belt, Int. J. Infect. Dis., Vol. 14, pp. e553-e559.

Sharomi, O. and Gumel, A.B. (2008). Curtailing smoking dynamics: A mathematical modeling approach, Appl. Math. Comput., Vol. 19, pp. 475-499.

Sharomi, O., Podder, C.N., Gumel, A.B., Elbasha, E.H. and Watmough, J. (2007). Role of incidence function in vaccine-induced backward bifurcation in some HIV models, Mathematical Biosciences, Vol. 210, No. 2, pp. 436-463.

Scherer, A. and McLean, A. (2002). Mathematical models of vaccination, British Medical Bulletin, Vol. 62, pp. 187-199.

Segal, S. and Pollard, A. J. (2004). Vaccines against bacterial meningitis, British Medical Bulletin, Vol. 72, No. 1, pp. 65-81.

Smith, H.L. and Waltman P. (1995). *The Theory of the Chemostat*, Cambridge University Press.

Stephens, D. S., Greenwood, B. and Brandtzaeg, P. (2007). Epidemic meningitis, meningococcaemia, and Neisseria meningitidis, Lancet (London, England), Vol. 369(9580), pp. 2196-2210.

Stollenwerk, N. and Jansen, V. A. (2003). Evolution towards criticality in an epidemiological model for meningococcal disease, Physics Letters A, Vol. 317, No. (1-2), pp. 87-96.

Sultan, B., Labadi, K., Guégan, J. F. and Janicot, S. (2005). Climate drives the meningitis epidemics onset in West Africa, PLoS Medicine, Vol. 2, No. 1, pp. e6.

Trotter, C. L., Gay, N. J. and Edmunds, W. J. (2005). Dynamic models of meningococcal carriage, disease, and the impact of serogroup C conjugate vaccination, American Journal of Epidemiology, Vol. 162, No. 1, pp. 89-100.

Trotter, C. L. and Greenwood, B. M. (2007). Meningococcal carriage in the African meningitis belt, The Lancet Infectious Diseases, Vol. 7, No. 12, pp. 797-803.

Tuckwel, H-C., Hanslik, T., Valleron, A-J., and Flahault A. (2003). A mathematical model for evaluating the impact of vaccination schedules: Application to Neisseria meningitidis, Epidemiol. Infect., Vol. 3, pp. 419-429.

Tzeng, Y. L. and Stephens, D. S. (2000). Epidemiology and pathogenesis of Neisseria meningitidis, Microbes and Infection, Vol. 2, No. 6, pp. 687-700.

Van den Driessche, P. and Watmough, J. (2002). Reproduction numbers and sub-threshold endemic equilibria for compartmental models of disease transmission, Mathematical Biosciences, Vol. 180, No. (1-2), pp. 29-48.

Varga, R.S. (1962). *Matrix Iterative Analysis*, Prentice Hall, Englewood Cliffs, New Jersey.

Teyssou, R. and Muros-Le Rouzic, E. (2007). Meningitis epidemics in Africa: A brief overview, Vaccine, Vol. 25, pp. A3-A7.

Thieme, H-R. (2003). *Mathematics in Population Biology*, Princeton, Series Theoretical Computational Biology, Princeton University Press, Princeton, NJ.

World Health Organization. (2009). Global Alert and Response: Meningococcal Disease: Situation in the African Meningitis Belt. 25 March 2009. [Accessed 6 July, 2010]. Available at http://www.who.int/csr/don/2009-03-25/en/index. html.

World Health Organization. (2010). Meningitis Fact sheet N 141. Revised February 2010. [Accessed 6 July, 2010]. Available at http://www.who.int/mediacentre/factsheets/fs141/en/.

World Health Organization. (2013). Weekly epidemiological record: Meningococcal disease in countries of the African meningitis belt, 2012 an emerging needs and future perspectives, Vol. 88, pp. 129-136. Available at http://www. who.int/wer.

World Health Organization. (2010). Global Alert and Response: Meeting the public health challenge of epidemic meningitis in Africa. Undated. [Accessed 6 July, 2010]. Available at http://www.who.int/csr/disease/meningococcal/ challenge2004-11-10/en/index.html.

Wilder-Smith, A. and Memish, Z. (2003). Meningococcal disease and travel, International Journal of Antimicrobial Agents, Vol. 21, No. 2, pp. 102-106.

Xu, C. (2013). Stability and bifurcation analysis in a viral model with delay, Mathematical Methods in the Applied Sciences, Vol. 36, No. 10, pp. 1310-1320.

Xu, C. and Li, P. (2015). Oscillations for a delayed predator-prey model with Hassell-Varley type functional response, Comptes Rendus Biologies, Vol. 338, No. 4, pp. 227-240.

Xu, C. and Liao, M. (2014). Bifurcation analysis of an autonomous epidemic predator-prey model with delay, Annali di Matematica Pura ed Applicata, Vol. 193, No. 1, pp. 23-38.

Appendix A: Proof of Theorem 3.4

We prove this theorem using a result by Castillo-Chavez and Song in Castillo-Chavez and Song (2004). To that end, we do the following change of variables: $x_1 = S$, $x_2 = V$, $x_3 = C$, $x_4 = I$ and $x_5 = R$ so that $N = x_1 + x_2 + x_3 + x_4 + x_5$. Moreover, we adopt the following notations:

$$x = (x_1, x_2, x_3, x_4, x_5); \quad h = (h_1, h_2, h_3, h_4, h_5) \quad \text{and} \qquad \lambda_h = \frac{\beta_h(\varepsilon x_3 + x_4)}{N}.$$

Then, system (6) takes the form:

$$\dot{x} = h(x), \tag{42}$$

with,

$$\begin{cases} h_1 = \Lambda + \omega x_2 - (\mu + \theta + (1 + \lambda_a^0)\lambda_h)\, x_1 + \varphi x_5, \\ h_2 = \theta x_1 - (\omega + \mu + (1 + \lambda_a^0)k_7\lambda_h)\, x_2, \\ h_3 = (((1-p)\lambda_a^0 + 1)\, x_1 + ((1-q)\lambda_a^0 + 1)\, k_7 x_2)\, \lambda_h - (\mu + \alpha + \gamma)\, x_3, \\ h_4 = (p x_1 + q k_7 x_2)\, \lambda_a^0 \lambda_h + \gamma x_3 - (\mu + d + \delta) x_4, \\ h_5 = \delta x_4 + \alpha x_3 - (\varphi + \mu) x_5. \end{cases}$$

The system (42) has a DFE given by $E^0 = (x_1^0, x_2^0, 0, 0, 0)$, where

$$x_1^0 = \frac{\Lambda(\mu + \omega)}{\mu(\mu + \omega + \theta)} \quad \text{and} \quad x_2^0 = \frac{\Lambda\theta}{\mu(\mu + \omega + \theta)}.$$

Next, we consider the case where $\mathcal{R}_0^{av} = 1$ and set, $\beta_h = \beta_h^{**}$ as the chosen bifurcation parameter. Solving $\mathcal{R}_0^{av} = 1$ gives

$$\beta_h = \beta_h^{**} = \frac{N^0 D_1 D_2}{(\varepsilon D_2 + \gamma)\, D_3 + D_1 D_4}.$$

The Jacobian matrix of system (42) at the DFE E^0 denoted by $J_{\beta_h^{**}}$ is given by Equation (16) in which β_h is replaced by β_h^{**}. Its characteristic polynomial takes the form:

$$Q(X) = -X\,(X + \mu + \varphi)\,(X + \Phi)\left(X^2 + (2\mu + \omega + \theta)\, X + \mu\,(\mu + \omega + \theta)\right),$$

where,

$$\Phi = \frac{D_1\,(\gamma D_3 + D_1 D_4) + D_2 D_3\,(\varepsilon D_2 + \gamma)}{(\varepsilon D_2 + \gamma)\, D_3 + D_1 D_4}.$$

It follows that $J_{\beta_h^{**}}$ has a simple zero eigenvalue, while the remaining eigenvalues have negative real parts. Hence, the Center Manifold theory (Carr (1981)) can be used to analyze the dynamics of system (42). In particular, a result in Castillo-Chavez and Song (2004), reproduced below for convenience, is used to prove that, when the requirements in Theorem 3.4 are met, there exists a unique endemic equilibrium of system (42) (as shown in Lemma 3.3), which is locally asymptotically stable for $\mathcal{R}_0^{av}$ greater than 1 but close to 1.

Theorem 5.1. (Castillo-Chavez and Song (2004))

Consider the following general system of ordinary differential equations with a parameter ϕ:

$$\frac{dz}{dt} = g(z, \phi), \quad g : \mathbb{R}^n \times \mathbb{R} \longrightarrow \mathbb{R} \quad and \quad g \in \mathcal{C}^2(\mathbb{R}^n, \mathbb{R}), \tag{43}$$

where 0 is an equilibrium point of the system (that is, $g(0,\phi) \equiv 0$ for all ϕ) and assume

(1) $M = D_z g(0,0) = \left(\frac{\partial g_i}{z_j}(0,0)\right)$ is the linearized matrix of system (42) around the equilibrium 0 with ϕ evaluated at 0. Zero is a simple eigenvalue of M and other eigenvalues of M have negative real parts;
(2) Matrix M has a right eigenvector u and a left eigenvector v (each corresponding to the zero eigenvalue).

Let g_k be the k^{th} component of g and

$$\mathcal{A} = \sum_{k,i,j=1}^{n} v_k u_i u_j \frac{\partial^2 g_k}{\partial z_i \partial z_j}(0,0),$$
$$\mathcal{B} = \sum_{k,i=1}^{n} v_k u_i \frac{\partial^2 g_k}{\partial z_i \partial \phi}(0,0).$$

Then, the local dynamics of the system around the equilibrium point 0 is totally determined by the signs of $\mathcal{A}$ and $\mathcal{B}$ as follows:

(i) $\mathcal{A} > 0$, $\mathcal{B} > 0$. When $\phi < 0$ with $\mid \phi \mid \ll 1$, 0 is locally asymptotically stable and there exists a positive unstable equilibrium; when $0 < \phi \ll 1$, 0 is unstable and there exists a negative, locally asymptotically stable equilibrium;
(ii) $\mathcal{A} < 0$, $\mathcal{B} < 0$. When $\phi < 0$ with $\mid \phi \mid \ll 1$, 0 is unstable; when $0 < \phi \ll 1$, 0 is locally asymptotically stable equilibrium, and there exists a positive unstable equilibrium;
(iii) $\mathcal{A} > 0$, $\mathcal{B} < 0$. When $\phi < 0$ with $\mid \phi \mid \ll 1$, 0 is unstable, and there exists a locally asymptotically stable negative equilibrium; when $0 < \phi \ll 1$, 0 is stable, and a positive unstable equilibrium appears;
(iv) $\mathcal{A} < 0$, $\mathcal{B} > 0$. When ϕ changes from negative to positive, 0 changes its stability from stable to unstable. Correspondingly a negative unstable equilibrium becomes positive and locally asymptotically stable.

Particularly, if $\mathcal{A} > 0$ and $\mathcal{B} > 0$, then a backward bifurcation occurs at $\phi = 0$.

In order to apply the above theorem, the following computations are necessary. We recall that β_h^{**} is the bifurcation parameter, in place of ϕ in Theorem (Castillo-Chavez and Song (2004)).

Eigenvectors of $J_{\beta_h^{**}}$: For the case when $\mathcal{R}_0^{av} = 1$, it can be shown that the Jacobian matrix $J_{\beta_h^{**}}$ of model system (42) at $\beta_h = \beta_h^{**}$ has a right eigenvector (corresponding to the zero eigenvalues),

given by $u = (u_1, u_2, u_3, u_4, u_5)$. Denote by $\Sigma^0_{**} = \beta^{**}_h/N^0$, we have:

$$u_1 = \left\{(\mu+\omega)\varphi u_5 - \Sigma^0_{**}\left(1+\lambda^0_a\right)(\varepsilon u_3 + u_4)\left((\mu+\omega)S^0 + \omega k_7 V^0\right)\right\}(\mu(\mu+\omega+\theta)),$$
$$u_2 = \left\{\theta\varphi u_5 - \Sigma^0_{**}\left(1+\lambda^0_a\right)(\varepsilon u_3 + u_4)\left(\theta S^0 + (\mu+\theta)k_7 V^0\right)\right\}(\mu(\mu+\omega+\theta)),$$
$$u_3 = \frac{(\mu+\varphi)D_2D_3}{D_3(\delta\gamma+\alpha D_2)+\delta D_1D_4}u_5, \quad u_4 = \frac{(\mu+\varphi)(\gamma D_3 + D_1D_4)}{D_3(\delta\gamma+\alpha D_2)+\delta D_1D_4}u_5, \ u_5 > 0.$$

Similarly, the components of the left eigenvectors of $J_{\beta^{**}_h}$ (corresponding to the zero eigenvalue), denoted by $v = (v_1, v_2, v_3, v_4, v_5)$, are given by,

$$v_1 = 0, \quad v_2 = 0, \quad v_3 > 0, \quad v_4 = \frac{D_1}{\varepsilon D_2 + \gamma}v_3 \quad \text{and} \quad v_5 = 0.$$

Computation of $\mathcal{B}$: For the sign of $\mathcal{B}$, it can be shown that the associated non-vanishing partial derivatives of h are

$$\frac{\partial^2 h_3}{\partial x_3 \partial \beta^{**}_h} = \frac{D_3}{N^0}, \quad \frac{\partial^2 h_3}{\partial x_4 \partial \beta^{**}_h} = \frac{D_3}{N^0} \quad \text{and} \quad \frac{\partial^2 h_4}{\partial x_3 \partial \beta^{**}_h} = \frac{\varepsilon D_4}{N^0}, \quad \frac{\partial^2 h_4}{\partial x_4 \partial \beta^{**}_h} = \frac{D_4}{N^0}.$$

Then, one has that

$$\mathcal{B} = v_3 \sum_{i=3}^{4} u_i \frac{\partial^2 h_3}{\partial x_i \partial \beta^{**}_h} + v_4 \sum_{i=3}^{4} u_i \frac{\partial^2 h_4}{\partial x_i \partial \beta^{**}_h} = \frac{(\varepsilon u_3 + u_4)(D_3 v_3 + D_4 v_4)}{N^0} > 0. \tag{44}$$

Computation of $\mathcal{A}$: For system (42), the associated nonzero partial derivatives of h (at the DFE E^0) are given by

$$\frac{\partial^2 h_3}{\partial x_1 \partial x_3} = \frac{((1-p)\lambda^0_a + 1)\varepsilon\beta^{**}_h}{N^0} - \frac{\beta^{**}_h \varepsilon D_3}{(N^0)^2}, \quad \frac{\partial^2 h_3}{\partial x_1 \partial x_4} = \frac{((1-p)\lambda^0_a + 1)\beta^{**}_h}{N^0} - \frac{\beta^{**}_h D_3}{(N^0)^2},$$

$$\frac{\partial^2 h_3}{\partial x_2 \partial x_3} = \frac{k_7((1-q)\lambda^0_a + 1)\varepsilon\beta^{**}_h}{N^0} - \frac{\beta^{**}_h \varepsilon D_3}{(N^0)^2}, \quad \frac{\partial^2 h_3}{\partial x_2 \partial x_4} = \frac{k_7((1-q)\lambda^0_a + 1)\beta^{**}_h}{N^0} - \frac{\beta^{**}_h D_3}{(N^0)^2},$$
$$\frac{\partial^2 h_3}{\partial x_3^2} = -\frac{2\beta^{**}_h \varepsilon D_3}{(N^0)^2}, \quad \frac{\partial^2 h_3}{\partial x_3 \partial x_4} = -\frac{\beta^{**}_h(1+\varepsilon)D_3}{(N^0)^2}, \quad \frac{\partial^2 h_3}{\partial x_3 \partial x_5} = -\frac{\beta^{**}_h \varepsilon D_3}{(N^0)^2}, \quad \frac{\partial^2 h_3}{\partial x_4^2} = -\frac{2\beta^{**}_h D_3}{(N^0)^2},$$
$$\frac{\partial^2 h_3}{\partial x_4 \partial x_5} = -\frac{\beta^{**}_h D_3}{(N^0)^2}, \quad \frac{\partial^2 h_4}{\partial x_1 \partial x_3} = \frac{p\lambda^0_a \varepsilon \beta^{**}_h}{N^0} - \frac{\beta^{**}_h \varepsilon D_4}{(N^0)^2}, \quad \frac{\partial^2 h_4}{\partial x_1 \partial x_4} = \frac{P\lambda^0_a \beta^{**}_h}{N^0} - \frac{\beta^{**}_h D_4}{(N^0)^2},$$
$$\frac{\partial^2 h_4}{\partial x_2 \partial x_3} = \frac{q\lambda^0_a k_7 \varepsilon \beta^{**}_h}{N^0} - \frac{\beta^{**}_h \varepsilon D_4}{(N^0)^2}, \quad \frac{\partial^2 h_4}{\partial x_4 \partial x_5} = -\frac{\beta^{**}_h D_4}{(N^0)^2}, \quad \frac{\partial^2 h_4}{\partial x_2 \partial x_4} = \frac{q\lambda^0_a k_7 \beta^{**}_h}{N^0} - \frac{\beta^{**}_h D_4}{(N^0)^2},$$
$$\frac{\partial^2 h_4}{\partial x_3^2} = -\frac{2\beta^{**}_h \varepsilon D_4}{(N^0)^2}, \quad \frac{\partial^2 h_4}{\partial x_3 \partial x_4} = -\frac{\beta^{**}_h(1+\varepsilon)D_4}{(N^0)^2}, \quad \frac{\partial^2 h_4}{\partial x_4^2} = -\frac{2\beta^{**}_h D_4}{(N^0)^2}, \quad \frac{\partial^2 h_4}{\partial x_3 \partial x_5} = -\frac{\beta^{**}_h \varepsilon D_4}{(N^0)^2}.$$

Then, setting $D_5 = u_1 + u_2 + u_3 + u_4 + u_5$, it follows that

$$\begin{aligned}\mathcal{A} &= v_3 \sum_{i,j=1}^{6} u_i u_j \frac{\partial^2 h_3}{\partial x_i \partial x_j} + v_4 \sum_{i,j=1}^{6} u_i u_j \frac{\partial^2 h_4}{\partial x_i \partial x_j}, \\ &= \frac{2\beta_h^* (u_3\varepsilon + u_4)}{N^0} \big\{ v_3 \left\{ u_1 \left((1-p)\lambda_a^0 + 1 \right) + u_2 k_7 \left((1-q)\lambda_a^0 + 1 \right) \right\} + v_4 \lambda_a^0 \left[u_1 p + u_2 q k_7 \right] \big\} \\ &\quad - \frac{2\beta_h^* (u_3\varepsilon + u_4) (v_3 D_3 + v_4 D_4) D_5}{(N^0)^2}.\end{aligned} \tag{45}$$

Thus, depending on the values of the parameters of system (6), the value of $\mathcal{A}$ can be positive or negative. So, since $\mathcal{B} > 0$, the conclusion follows from Theorem 5.1 items (i) and (iv).